Molecular Therapy
Oncolytics
Original Article

Superior infectivity of the fiber chimeric oncolytic adenoviruses Ad5/35 and Ad5/3 over Ad5-delta-24-RGD in primary glioma cultures

Aleksei A. Stepanenko,[1,2] Anastasiia O. Sosnovtseva,[1] Marat P. Valikhov,[1,2] Anastasia A. Chernysheva,[1] Sergey A. Cherepanov,[1] Gaukhar M. Yusubalieva,[3] Zsolt Ruzsics,[4,5] Anastasiia V. Lipatova,[6] and Vladimir P. Chekhonin[1,2]

[1]Department of Fundamental and Applied Neurobiology, V.P. Serbsky National Medical Research Center of Psychiatry and Narcology, The Ministry of Health of the Russian Federation, Kropotkinsky Lane 23, 119034 Moscow, Russia; [2]Department of Medical Nanobiotechnology, Institute of Translational Medicine, N.I. Pirogov Russian National Research Medical University, The Ministry of Health of the Russian Federation, Ostrovitianov Str. 1, 117997 Moscow, Russia; [3]Federal Research and Clinical Center for Specialized Types of Medical Care and Medical Technologies of the FMBA of Russia, Moscow, Russia; [4]Institute of Virology, Medical Center, University of Freiburg, Freiburg, Germany; [5]Faculty of Medicine, University of Freiburg, Freiburg, Germany; [6]Center for Precision Genome Editing and Genetic Technologies for Biomedicine, Engelhardt Institute of Molecular Biology, Russian Academy of Sciences, Moscow, Russia

Ad5-delta-24-RGD is currently the most clinically advanced recombinant adenovirus (rAd) for glioma therapy. We constructed a panel of fiber-modified rAds (Ad5RGD, Ad5/3, Ad5/35, Ad5/3RGD, and Ad5/35RGD, all harboring the delta-24 modification) and compared their infectivity, replication, reproduction, and cytolytic efficacy in human and rodent glioma cell lines and short-term cultures from primary gliomas. In human cells, both Ad5/35-delta-24 and Ad5/3-delta-24 displayed superior infectivity and cytolytic efficacy over Ad5-delta-24-RGD, while Ad5/3-delta-24-RGD and Ad5/35-delta-24-RGD did not show further improvements in efficacy. The expression of the adenoviral receptors/coreceptors CAR, DSG2, and CD46 and the integrins αVβ3/αVβ5 did not predict the relative cytolytic efficacy of the fiber-modified rAds. The cytotoxicity of the fiber-modified rAds in human primary normal cultures of different origins and in primary glioma cultures was comparable, indicating that the delta-24 modification did not confer tumor cell selectivity. We also revealed that CT-2A and GL261 glioma cells might be used as murine cell models for the fiber chimeric rAds *in vitro* and *in vivo*. In GL261 tumor-bearing mice, Ad5/35-delta-24, armed with the immune costimulator OX40L as the E2A/DBP-p2A-mOX40L fusion, produced long-term survivors, which were able to reject tumor cells upon rechallenge. Our data underscore the potential of local Ad5/35-delta-24-based immunovirotherapy for glioblastoma treatment.

INTRODUCTION

Despite aggressive multimodal therapy (surgery, radiation, chemotherapy, and investigational drugs), the median survival rate of adult patients with newly diagnosed and recurrent glioblastoma (WHO grade IV malignant glioma) is usually no more than 18–20 months and 8–12 months, respectively.[1] Over the past decade, high expectations have been placed on targeted therapies to control tumor growth and to further improve survival. However, to date, targeted chemotherapeutics or antibodies have not shown a greater efficacy than the standard genotoxic drug temozolomide or improved the efficacy of radiochemotherapy in patients with glioblastoma in clinical trials.[1] The high failure rate of trials and the lack of effective targeted therapy on the horizon have fueled the development of conceptually distinct therapeutic approaches, such as oncolytic virotherapy.[2,3]

Among the many different oncolytic viruses, recombinant adenoviruses (rAds) based on the human adenovirus 5 genome (Ad5) have been the most commonly used across many cancer types, including high-grade glioma.[4,5] In a phase I trial, the current mainstream oncolytic Ad5-delta-24-RGD (DNX-2401) induced a clinically relevant objective response and long-term survival (>3 years) in a fraction of patients with recurrent high-grade glioma, with no dose-limiting toxicities and no maximum tolerated dose found, and altered the immune tumor microenvironment promoting infiltration of CD8+ T cells and M1-polarized macrophages.[6,7] Ad5-delta-24-RGD has a 24-base pair deletion in a sequence encoding the conservative region 2 (CR2) domain of the E1A protein (delta-24, or Δ24), which binds SUMO-conjugase UBC9,[8] the stimulator of interferon genes (STING),[9] and the tumor-suppressor retinoblastoma protein (pRb).[10,11] In normal nonproliferating cells with intact pRb, replication of Ad5 with the delta-24 modification was shown to be

Received 3 May 2021; accepted 17 December 2021;
https://doi.org/10.1016/j.omto.2021.12.013.

Correspondence: Aleksei A. Stepanenko, Department of Fundamental and Applied Neurobiology, V.P. Serbsky National Medical Research Center of Psychiatry and Narcology, The Ministry of Health of the Russian Federation, Kropotkinsky Lane 23, 119034 Moscow, Russia.
E-mail: a.a.stepanenko@gmail.com

significantly attenuated.[10,11] However, these initial findings have not been recapitulated by other groups.[12–17]

The attachment of wild-type Ad5 to the host cell surface is mediated by the interaction of the fiber knob domain with coxsackievirus and adenovirus receptor (CAR), while virus internalization and endosome escape require the interaction of the arginine-glycine-aspartic acid (RGD)-motif containing loop of the penton base protein with cellular integrins, mainly αVβ3 and αVβ5.[18] However, the expression of CAR in glioma tissues and short-term cultures was frequently barely detectable.[19–22] CAR-negative/low cells are generally poorly infected with fiber nonmodified Ad5, although there are exceptions.[22–25] Ad5-delta-24-RGD harbors an RGD motif-containing integrin-targeting peptide (RGD-4C)[26] in the HI loop of the fiber knob domain that substantially improves the transduction efficacy in CAR-negative/low cell lines and the therapeutic efficacy in *in vivo* models.[27–30]

Another strategy to improve the infectivity of Ad5-based rAds is fiber knob serotype switching, which is achieved by constructing chimeric fibers consisting of the knob domain (and the shaft domain in some cases) derived from an alternate adenoviral serotype.[3] Although the fiber knob domains from different human and nonhuman adenoviruses were tested for their ability to increase the transduction efficacy in tumor cells,[31] the most advanced preclinical/clinical fiber chimeric rAds are Ad5/3- and Ad5/35-based.[32] Ad3 utilizes desmoglein 2 (DSG2) as a primary high-affinity receptor[33] and CD46 as a low-affinity receptor (avidity-binding),[34] while Ad35 uses CD46 as a primary high-affinity receptor.[35] DSG2 and CD46 expression is preserved in tumor cells,[36] including glioma tissues.[19] Importantly, the transduction and cytolytic efficacy of Ad5/3 were superior to those of Ad5RGD in different cancer cell types.[37–43] Similarly, the transduction efficacy of the Ad5/35 reporter virus was higher than that of Ad5RGD in several tested cancer cell types,[44–46] including glioma.[46] To further increase the transduction efficacy of fiber chimeric Ad5/3-based rAds, an approach (complex fiber mosaicism) combining serotype fiber chimerism with the incorporation of a targeting peptide into the chimeric fiber has been proposed.[42,47,48]

To evaluate the relative infectivity, replication, reproduction, and cytolytic efficacy of the fiber-modified replication-competent rAds, we constructed Ad5RGD, Ad5/3, Ad5/3RGD, Ad5/35, and Ad5/35RGD (all harboring the *E1A*Δ24 modification) and comprehensively compared their activity in established human and rodent glioma cell lines, human short-term primary glioma cultures, human primary normal cell cultures of different origins, and immunocompetent murine glioma models.

RESULTS

Construction of the fiber-modified replication-competent rAds

To construct a panel of the fiber-modified replication-competent rAds, we cloned the wild-type Ad5 genome into a predesigned pSC101-CmR plasmid and then verified its integrity and forward orientation by restriction enzyme digests (Figure S1). Furthermore, we deleted 24-base pairs within the *E1A* gene in the Ad5 genome at 922–947 bp corresponding to amino acids 122-LTCHEAGF-129 in the CR2 domain of the E1A protein in order to obtain Ad5-Δ24[10,11] (Figure S2A), from which the fiber-modified rAds were derived. The following set of fiber-modified rAds was constructed (summarized in Figures S2B–S2D): Ad5-Δ24-RGD with the RGD-4C peptide (ACDCRGDCFCG) inserted into the HI loop of the fiber knob between amino acids 546 and 547;[27] Ad5/3-Δ24 with the fiber knob domain derived from Ad3;[49] Ad5/35-Δ24 with the fiber shaft and knob domains derived from Ad35;[50] and Ad5/3-Δ24-RGD and Ad5/35-Δ24-RGD with the RGD-4C peptide fused to the C termini of the corresponding chimeric fibers via a glycine-serine 3×(GGGGS) linker sequence to increase accessibility and conformational flexibility.[42,47,48,51] The replication-defective Ad5ΔE1A virus was obtained by deleting the entire coding sequence for the E1A protein (data not shown). The physical (viral particle [vp]/mL) and infectious (infectious unit [IFU]/mL) titers of rAd preparations and their ratios are provided in Table S1. The restriction enzyme digestion patterns verified the genomic integrity of the rescued purified rAds (Figure S3).

Comparative transduction, replication, reproduction, and cytolytic efficacy of the fiber-modified rAds in human cell cultures

We first tested the fiber-modified rAds in LN18, LN229, and DBTRG glioma and in A549 lung adenocarcinoma cell lines using a qualitative crystal violet cell viability assay (Figure S4). Ad5-Δ24-RGD was more effective than parental Ad5-Δ24 with the wild-type fiber in the majority of the tested cell lines (Figure S4A). Depending on the cell line, Ad5/3-Δ24-RGD showed similar or inferior cytolytic efficacy compared with the parental Ad5/3-Δ24 (Figure S4B), while Ad5/35-Δ24-RGD was severely defective compared with the parental Ad5/35-Δ24 in all of the tested cell lines (Figure S4C). No less than 500 vp/cell of Ad5/35-Δ24-RGD was required for A549 and LN18 cells to induce the cytopathic effect at day 8 post-infection (Figure S4D). In the quantitative resazurin/Alamar Blue cell viability assay, Ad5/3-Δ24 was more efficient than Ad5-Δ24-RGD in LN18, LN229, DBTRG, and A549 cells, while Ad5/35-Δ24 was more potent than Ad5-Δ24-RGD in LN18, LN229, and T98G cells (Figures 1A and S4E). These observations were reproduced using other large-scale virus preparations (50% inhibition [IC50] values in Table S2). We also confirmed that two independently rescued and purified clones of Ad5/3-Δ24-RGD were generally less effective than parental Ad5/3-Δ24 in glioma cell lines (Figure S4F).

To validate the superior efficiency of fiber chimeric Ad5/35-Δ24 and Ad5/3-Δ24, we constructed the fiber-modified rAds expressing firefly luciferase (Fluc) fused through a p2A sequence (ATNFSLLKQAGDVEENPGP with a GSG linker) to the C termini of the corresponding viral proteins (E1B or E2A/DBP). However, only the resultant rAds with the E1B-p2A-Fluc fusion could be readily rescued, while several attempts to rescue two clones of rAds with the DBP-p2A-Fluc fusion were unsuccessful for an unknown reason. In contrast, Ad5/35-Δ24 with the DBP-p2A-EGFP or DBP-p2A-murine OX40 ligand (mOX40L) fusions was successfully rescued and amplified with similar growth kinetics compared with the parental Ad5/35-Δ24

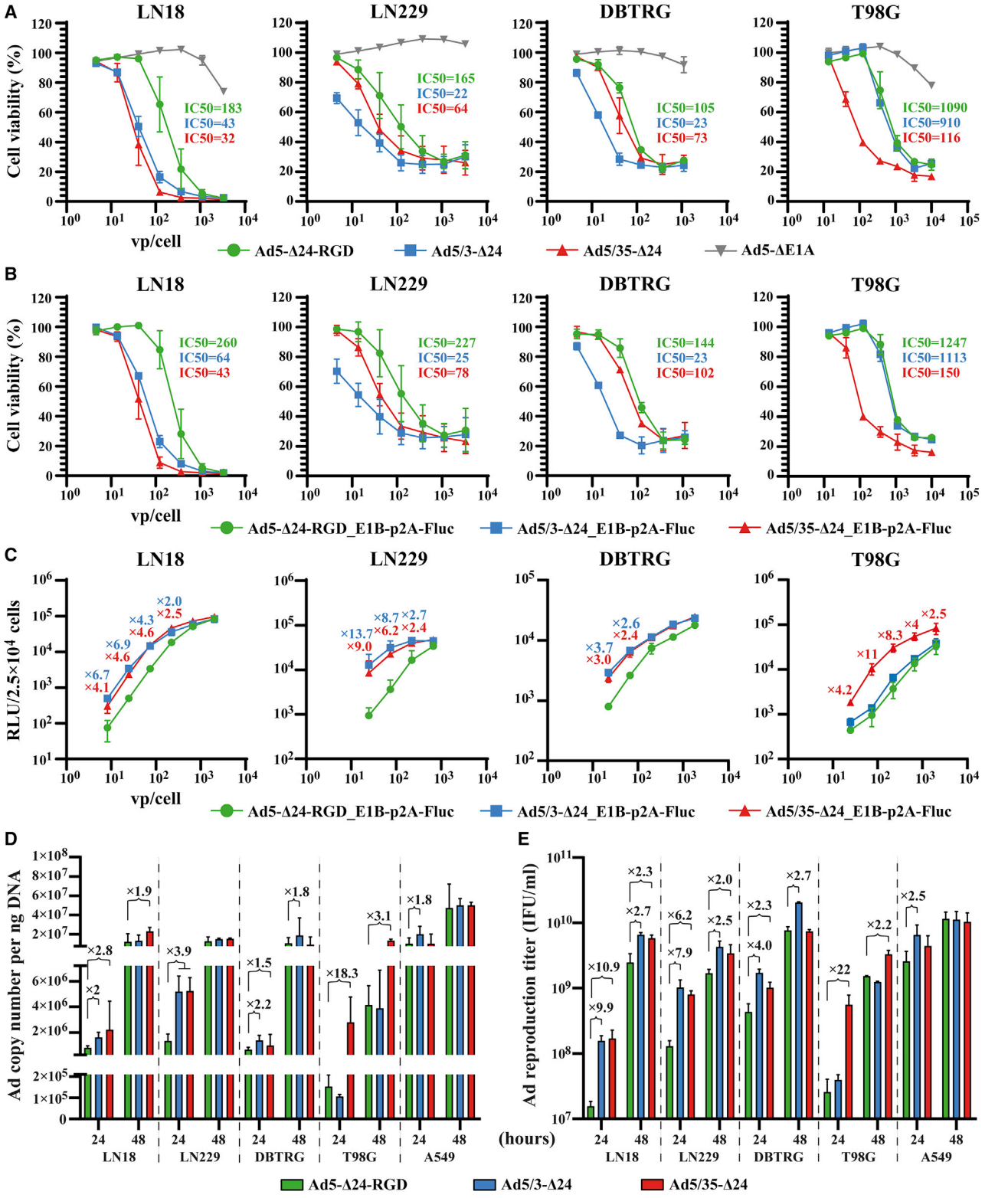

(legend on next page)

(discussed below). The comparative cytolytic efficacy of the fiber-modified rAds expressing Fluc was consistent with the corresponding fiber-modified rAd counterparts not encoding the reporter transgene (Figures 1B and S4G). The greater cytotoxicity of fiber-chimeric Ad5/35-Δ24 and Ad5/3-Δ24 compared with Ad5-Δ24-RGD in the tested cell lines could be explained by the strong differences in their infectivity, which was assessed by analysis of Fluc activity 24 h post-infection (Figures 1C and S4H).

We next evaluated the replication potential of the fiber-modified rAds in human glioma cell lines. Quantification of the viral DNA copies confirmed the ability of the fiber-modified rAds to efficiently replicate (Figure 1D). However, Ad5/3-Δ24 and Ad5/35-Δ24 generally outperformed Ad5-Δ24-RGD. Finally, the fiber chimeric Ad5/3-Δ24 and/or Ad5/35-Δ24 produced more viral progeny than Ad5-Δ24-RGD, especially 24 h post-infection (Figure 1E). Thus, Ad5/3-Δ24 and Ad5/35-Δ24 showed generally superior infectivity over Ad5-Δ24-RGD and, as a result, more potent relative replication, reproduction, and cytotoxicity in glioma cell lines, while fusing the RGD-4C peptide to the C terminus of the chimeric fiber via a linker did not improve the oncolytic efficacy of Ad5/3-Δ24-RGD but rather impaired it, especially in the case of Ad5/35-Δ24-RGD.

To further confirm the relevance of our findings, we compared the cytolytic efficacy of Ad5-Δ24-RGD, Ad5/3-Δ24, and Ad5/35-Δ24 in short-term primary glioma (n = 8) and medulloblastoma (n = 1) cultures (Figure 2). GliSav glioma culture was the only cell culture abundantly available for the additional comparative cell viability experiments (Figure S5A) due to a relatively fast proliferation rate, while all other short-term cultures showed slow/very slow cycling. We found that Ad5/35-Δ24 was significantly more effective (>5-fold difference in the IC50 values as a criterion) than Ad5-Δ24-RGD in five cultures (Figures 2A, 2C, 2D, 2G, 2I, and S5B) and was more effective than Ad5/3-Δ24 in two cultures (Figures 2A, 2I, and S5B). Ad5/3-Δ24 was more effective than Ad5-Δ24-RGD in four cultures (Figures 2C, 2D, 2F, 2G, and S5B) and was more effective than Ad5/35-Δ24 in one culture (Figures 2F and S5B). Ad5-Δ24-RGD was more effective than Ad5/3-Δ24 in one culture (Figures 2A and S5B) and was not more effective than Ad5/35-Δ24 in any culture. Thus, both Ad5/3-Δ24 and Ad5/35-Δ24 were generally more potent than clinically advanced Ad5-Δ24-RGD in short-term primary glioma cultures.

Finally, we compared the cytotoxicity of Ad5-Δ24-RGD, Ad5/3-Δ24, and Ad5/35-Δ24 in short-term primary normal cultures, which included human embryonic fibroblasts (HEFs), olfactory ensheathing cells (OECs), human aortic vascular smooth muscle cells (HA-VSMCs), human umbilical vein endothelial cells (HUVECs), and embryonic astrocytes (Figure 3). HEFs and OECs were largely refractory to Ad5-Δ24-RGD in a tested range of doses (100–0.01 vp/cell) (Figure 3A). Ad5/3-Δ24 was more cytotoxic than Ad5/35-Δ24 in HEFs and vice versa in OECs (Figure 3A). In the rest of the cell cultures, the relative cytotoxicity was ranked as follows (>5-fold difference in the IC50 values as a criterion): Ad5/35-Δ24 ≈ Ad5-Δ24-RGD > Ad5/3-Δ24 in HA-VSMCs, Ad5-Δ24-RGD ≈ Ad5/35-Δ24 > Ad5/3-Δ24 in HUVECs, and Ad5/35-Δ24 ≈ Ad5/3-Δ24 > Ad5-Δ24-RGD in embryonic astrocytes (Figure 3B). Importantly, the cytotoxicity of the fiber-modified rAds in proliferating primary normal cells and short-term glioma cultures was comparable (Figure S5B) despite the presence of the *E1A*Δ24 modification. Overall, although the relative cytotoxicity of the fiber-modified rAds was cell-type-dependent, Ad5/35-Δ24 and Ad5/3-Δ24 were generally more cytotoxic than Ad5-Δ24-RGD in proliferating primary normal cultures, and the *E1A*Δ24 modification by itself did not confer tumor cell selectivity.

The expression levels of known adenoviral receptors/coreceptors are not predictive of the relative oncolytic efficacy of the fiber-modified rAds

Next, we investigated whether the expression levels (percentage of positive cells) of known adenoviral receptors/coreceptors may predict the relative oncolytic efficacy (based on the IC50 values) of the fiber-modified rAds within each individual cell culture. We analyzed the expression of adenoviral receptors (CAR, DSG2, and CD46) and coreceptors (integrins αVβ3 and αVβ5) in established cell lines (n = 5), short-term primary glioma cell cultures (n = 5), and primary normal cell cultures (n = 2) (Figures 4 and S6–S8; Table S3). CAR expression varied from a low (≈8%) to high (≈98%) levels in established cell lines, while it was undetectable in short-term glioma cultures, HUVECs, and embryonic astrocytes. Similarly, DSG2 expression

Figure 1. The comparative infectivity, replication, reproduction, and cytolytic efficacy of the fiber-modified replication-competent recombinant adenoviruses in human glioma cell lines

(A and B) Comparative dose-dependent cytotoxicity. Cells (5×10^3/well) were infected in suspension with a serial 3-fold dilution of the indicated fiber-modified (A) and fiber-modified luciferase-expressing (B) rAds starting from 20,000 vp/cell (T98G cells), 6,666 vp/cell (LN18 and LN229), or 2,222 vp/cell (DBTRG) and analyzed 5 or 7 (T98G cells) days post-infection by resazurin/Alamar Blue cell viability assays. Replication-defective Ad5ΔE1A was used as a negative control. Normalized data are presented as the mean ± SD of at least two independent experiments in technical triplicates. (C) Comparative dose-dependent infectivity. Cells (2.5×10^4/well) were infected in suspension with a serial 3-fold dilution of the indicated luciferase-expressing rAds starting from 2,222 vp/cell or 741 vp/cell (LN229). Luminescence (relative light units [RLU]) was analyzed 24 h post-infection. Only ≥2-fold differences in the mean RLU values relative to Ad5-Δ24-RGD_E1B-p2A-Fluc are designated. The mean ± SD of two independent experiments in four technical replicates is shown. (D) Ad DNA copy number quantification by qPCR. Cells (5×10^5/well) were infected in suspension with 100 vp/cell and collected 24 and 48 h post-infection. Normalized data are shown as the mean ± SD of at least two independent experiments. PCR runs were conducted in four technical replicates. Only ≥1.5-fold differences in the mean DNA copy numbers relative to Ad5-Δ24-RGD are designated. (E) Total virus production (both culture cell extracts and supernatants including viral inoculum) was determined 24 and 48 h post-infection using anti-Ad staining. Cells (2.5×10^5/well) were infected in suspension at an MOI of 50 IFU/cell. The mean ± SD of two independent experiments is shown. Only ≥2-fold differences in the mean total virus production values (IFU/mL) relative to Ad5-Δ24-RGD are designated. See also Figure S4.

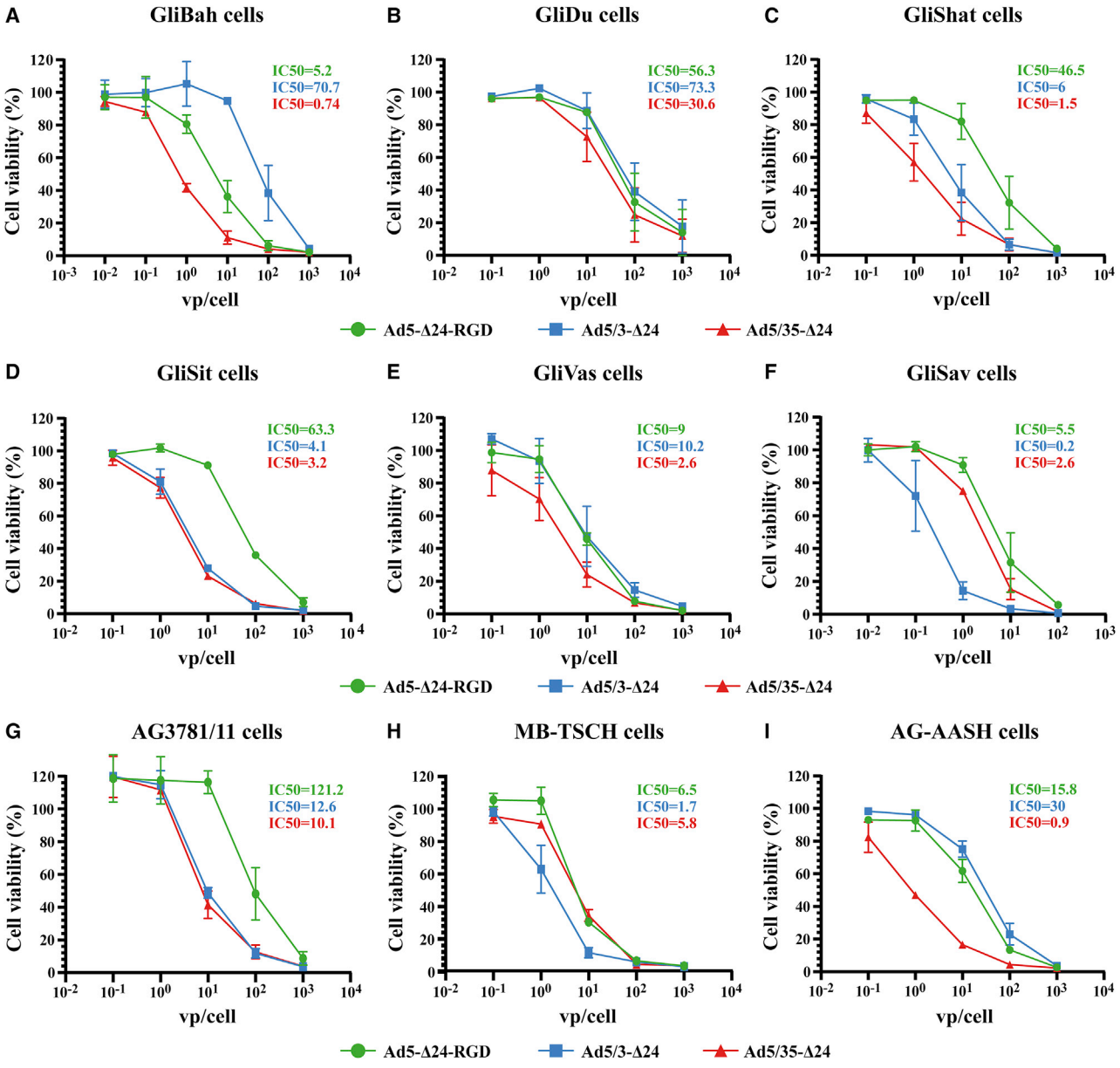

Figure 2. The comparative cytolytic efficacy of the fiber-modified replication-competent recombinant adenoviruses in human primary short-term glioma (n = 8) and medulloblastoma (n = 1, MB-TSCH) cultures

(A–I) Resazurin/Alamar Blue cell viability assays of rAd-infected short-term glioma cell cultures 7 days post-infection (except GliBah, 6 days post-infection). The glioma cultures (5×10^3 cells/well) were infected in suspension with a serial 10-fold dilution of the indicated rAds starting from 1,000 vp/cell. Normalized data are presented as the mean ± SD of two independent experiments in technical triplicates. See also Figure S5.

varied from a low (≈6%) to a high (>95%) level in established cell lines, while it was largely undetectable in short-term cell cultures, except GliSav (>80%) and embryonic astrocytes (≈70%). CD46 was expressed abundantly in all the tested cell cultures (≥85%). Integrin αVβ3 was not expressed in four short-term glioma cultures and was barely detectable in A549 cells (<5%), while integrin αVβ5 expression was detected at low (≈10%) to high (≈95%) levels in all of the tested cultures.

We revealed that the expression levels of known adenoviral receptors/coreceptors did not universally predict the relative cytolytic efficacy of the fiber-modified rAds in each individual cell culture (Figure 4). For instance, Ad5-Δ24-RGD was the least potent in LN18 cells despite the high expression levels of CAR and integrins. A549 cells were relatively less permissive to Ad5-Δ24-RGD and Ad5/35-Δ24 despite the high expression levels of CAR, CD46, and integrin αVβ5. Ad5-Δ24-RGD was as effective as Ad5/35-Δ24 in GliSav culture despite barely

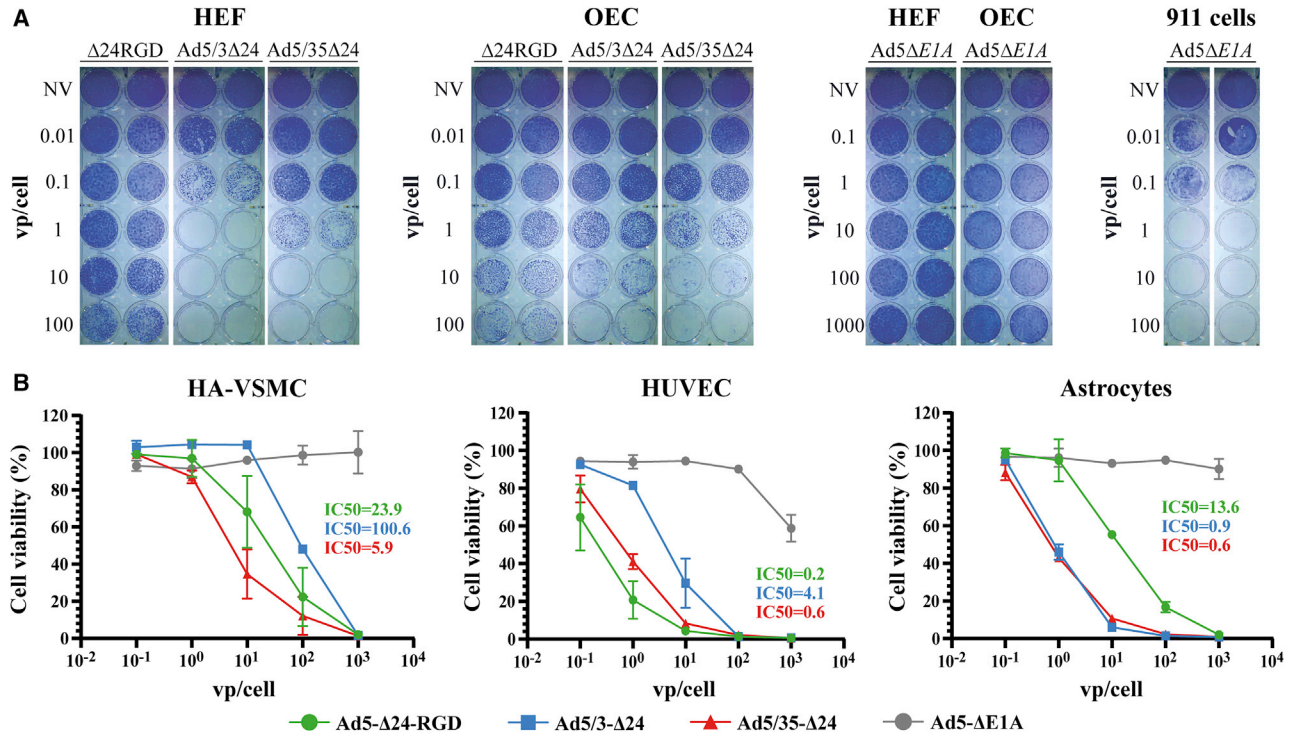

Figure 3. The comparative cytotoxicity of the fiber-modified replication-competent recombinant adenoviruses in human primary normal cells of different origins

(A) Crystal violet cell viability assays of rAd-infected primary human embryonic fibroblasts (HEFs) and olfactory ensheathing cells (OECs) 7 days post-infection. Cells (2.5×10^4/well) were infected in suspension with a serial 10-fold dilution of the indicated rAds starting from 100 vp/cell. Infection with a 10-fold serial dilution of the replication defective Ad5ΔE1A starting from 1,000 vp/cell was used as a negative control. The 911 cells were used as a positive control for replication-defective Ad5ΔE1A. Representative pictures of two independent experiments in technical duplicates with similar results are shown. (B) Resazurin/Alamar Blue cell viability assays of rAd-infected human primary aortic vascular smooth muscle cells (HA-VSMCs), umbilical vein endothelial cells (HUVECs), and embryonic astrocytes 7 days post-infection. Cells (5×10^3/well) were infected in suspension with a serial 10-fold dilution of the indicated rAds starting from 1,000 vp/cell. Normalized data are presented as the mean ± SD of two independent experiments in technical triplicates. See also Figure S5.

detectable CAR and integrin αVβ3 expression and low integrin αVβ5 expression. Ad5/3-Δ24 relatively efficiently killed GliShat cells despite a barely detectable level of DSG2 expression. Finally, we observed that Ad5/3-Δ24 outperformed Ad5/35-Δ24 in LN229, DBTRG, A549, and GliSav, which were found to express moderate to high levels of DSG2, although in embryonic astrocytes with high DSG2 expression, Ad5/3-Δ24 and Ad5/35-Δ24 were equally cytotoxic. Thus, based solely on the expression levels of known adenoviral receptors/coreceptors, it was not possible to positively predict which the fiber-modified rAds would be the most or least cytolytic in each individual cell culture.

CT-2A and GL261 glioma cells may be used as murine cell models for fiber chimeric rAds

To identify a rodent cell line that would be the most susceptible to Ad5/3-Δ24 and/or Ad5/35-Δ24 infection for further *in vivo* studies, we compared the cytotoxicity of the fiber-modified rAds in rodent glioma and carcinoma cell lines, which included GL261 and CT-2A murine glioma cells, C6 rat glioma cells, 4T1 murine mammary carcinoma cells, CT26 murine colon carcinoma cells, and B16-F10 murine melanoma cells (Figure 5). Rodent glioma and carcinoma cells exhibited cell line-specific sensitivity to the fiber-modified rAds. Ad5-Δ24-RGD outperformed parental Ad5-Δ24 in all of the tested rodent cell lines. CT-2A, C6, and 4T1 cells were the most sensitive to Ad5-Δ24-RGD (Figures 5B–5D). GL261 and C6 cells were the most sensitive to Ad5/3-Δ24 and Ad5/3-Δ24-RGD (Figures 5A and 5C), while other cell lines were almost refractory to these rAds in a tested range of viral doses. GL261 and CT-2A cells were the most sensitive to Ad5/35-Δ24 (Figures 5A and 5B). Interestingly, Ad5/35-Δ24 was as cytotoxic as Ad5-Δ24-RGD in GL261 cells (Figure 5A). Consistent with the crystal violet cell viability assays, different sensitivities of the rodent glioma cell lines to the fiber-modified rAds were observed in the resazurin/Alamar Blue cell viability assays (Figures 5G–5I). CT-2A cells were more sensitive to Ad5-Δ24-RGD than GL261 cells, while GL261 cells were more sensitive to Ad5/35-Δ24 than CT-2A cells (Figures 5G, 5H, and S10). Of note, we confirmed that Ad5/35-Δ24 and Ad5-Δ24-RGD had the same cytotoxicity in GL261 cells (Figure 5G).

To further substantiate the feasibility of murine glioma cell lines for the fiber chimeric rAds, we compared the cytotoxicity of the

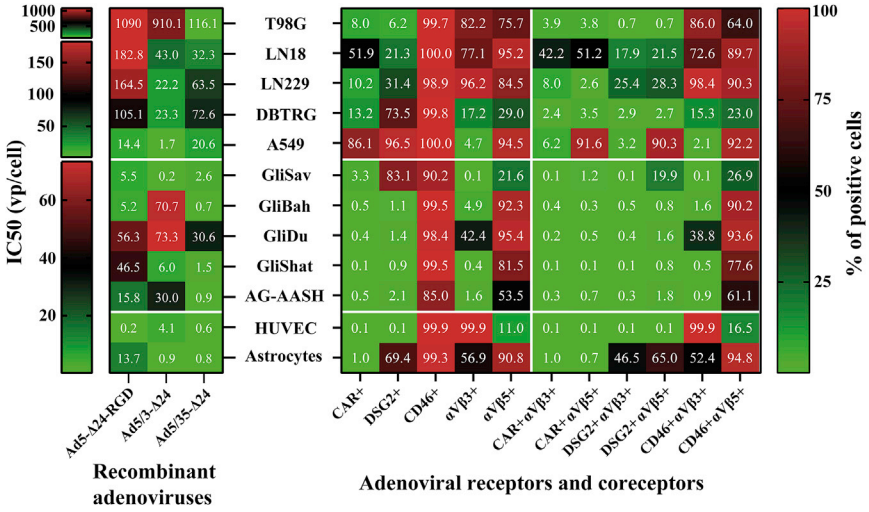

Figure 4. The expression levels of known adenoviral receptors and coreceptors in the established cell lines and the short-term primary cultures did not predict the relative oncolytic efficiency of the fiber-modified recombinant adenoviruses

The oncolytic efficacy represented by the IC50 values (vp/cell) for the indicated rAds (left panel) and the surface expression of receptors/coreceptors (percentage of positive cells, right panel) analyzed by flow cytometry are plotted as a heatmap. The IC50 values of rAds for established glioma cell lines and short-term primary glioma or normal cultures were derived from the resazurin/Alamar Blue cell viability assays 5 (except T98G, 7 days) and 7 days (except GliBah, 6 days) post-infection, respectively. Therefore, the three scale bars of the IC50 values are shown reflecting different readout time points in the cell viability assays. See also Figures S6–S8 and Table S3 for flow cytometry plots and statistics.

fiber-modified rAds expressing Fluc and revealed that their relative cytotoxic efficacy was consistent with that of the corresponding fiber-modified rAd counterparts not encoding the reporter transgene (Figure 6A). Surprisingly, despite a higher resistance (based on the IC50 values) of CT-2A cells to Ad5/35-Δ24_E1B-p2A-Fluc and Ad5/3-Δ24_E1B-p2A-Fluc compared with GL261 cells, these rAds (as well as Ad5-Δ24-RGD_E1B-p2A-Fluc) infected CT-2A cells more efficiently in a dose-dependent manner (Figure 6B): 5- to 49-fold on average for Ad5-Δ24-RGD_E1B-p2A-Fluc, 2- to 6-fold for Ad5/3-Δ24_E1B-p2A-Fluc, and 4-to 8-fold for Ad5/35-Δ24_E1B-p2A-Fluc (if comparing the relative light unit [RLU] values for each viral dose between cell lines). To independently confirm this observation, we constructed Ad5-Δ24-RGD_E1B-p2A-EGFP-, Ad5/35-Δ24_E1B-p2A-EGFP-, and Ad5/35-Δ24_DBP-p2A-EGFP-expressing EGFP fused through a p2A sequence to the C termini of the corresponding viral proteins (E1B or E2A/DBP). As expected, all of these rAds were equally cytotoxic in GL261 cells, and the Ad5/35-Δ24-based viruses expressing EGFP were more cytotoxic in GL261 cells than in CT-2A cells (Figure 6C). However, the flow cytometric analysis of Ad5/35-Δ24_DBP-p2A-EGFP-infected cells consistently showed that CT-2A cells were more efficiently infected than GL261 cells (Figure 6D). The higher activity of the reporter Fluc and EGFP transgenes in CT-2A cells compared with GL261 cells could be explained by a 101- to 452-fold higher number on average of viral DNA copies detected 24 h post-infection with the fiber-modified rAds (Figure 6D). We detected no further significant increase in DNA copy number in CT-2A cells 48 (Figure 6D) or 72 h (data not shown) post-infection. In contrast, the fiber-modified rAds efficiently replicated in GL261 cells (102- to 289-fold change on average, 72 versus 24 h; Figure 6D). The fiber-modified rAds were unable to produce viral progeny in either of the murine cell lines tested (Figure 6E). Finally, we compared the bioluminescence of syngeneic orthotopic GL261 and CT-2A gliomas infected with a single injection dose (5×10^9 vp) of the fiber-modified rAds using an *in vivo* imaging system (IVIS). Comparing the activity of Fluc between rAds within each glioma model, we found that the total luminescence on average from the Ad5/35-Δ24_E1B-p2A-Fluc-treated mice bearing GL261 gliomas was slightly but significantly higher than that of Ad5-Δ24-RGD_E1B-p2A-Fluc ($p = 0.0344$, two-way ANOVA with Tukey's multiple comparison test), while Ad5/3-Δ24_E1B-p2A-Fluc was more potent than Ad5/35-Δ24_E1B-p2A-Fluc in the CT-2A glioma model ($p = 0.0046$, two-way ANOVA with Turkey's multiple comparison test) (Figure S10). Moreover, comparing the activity of Fluc for each rAd between glioma models, we found a significant difference for Ad5/35-Δ24_E1B-p2A-Fluc ($p = 0.0022$, two-way ANOVA with Tukey's multiple comparison test), which was 2.2- to 3.4-fold on average more active in the GL261 glioma model 72 h and later post-infection (Figure 6G). The shortcoming of this experiment with the rAds expressing Fluc is that the total bioluminescent signal was apparently collected not only from infected glioma cells but also from infected normal cells, since the sham control animals (Figure 6G) who received an injection of Ad5/35-Δ24_E1B-p2A-Fluc also produced similar Fluc signals with regard to the average value and duration compared with those of the GL261 glioma model ($p = 0.5058$), but the values were still higher than those in the CT-2A glioma model ($p = 0.0083$, two-way ANOVA with Turkey's multiple comparison test). Currently, we have no explanation for these moderate differences in infectivity *in vivo* between the fiber-modified rAds and between the murine glioma models. We believe that these differences may actually be neglected in nonpermissive murine immune-competent orthotopic glioma models when high viral doses are administered several times for therapeutic purposes and due to a primary role of immune responses in the therapeutic efficacy of oncolytic viruses.

Characterization of the Ad5/35-Δ24_E1B-p2A-EGFP and Ad5/35-Δ24_DBP-p2A-EGFP oncolytic adenoviruses

According to our data, GL261 cells may be potentially used as a murine glioma model for Ad5/35-based rAds. However, it was previously shown that intratumoral administration of clinically advanced Ad5-Δ24-RGD alone was not sufficient to produce long-term

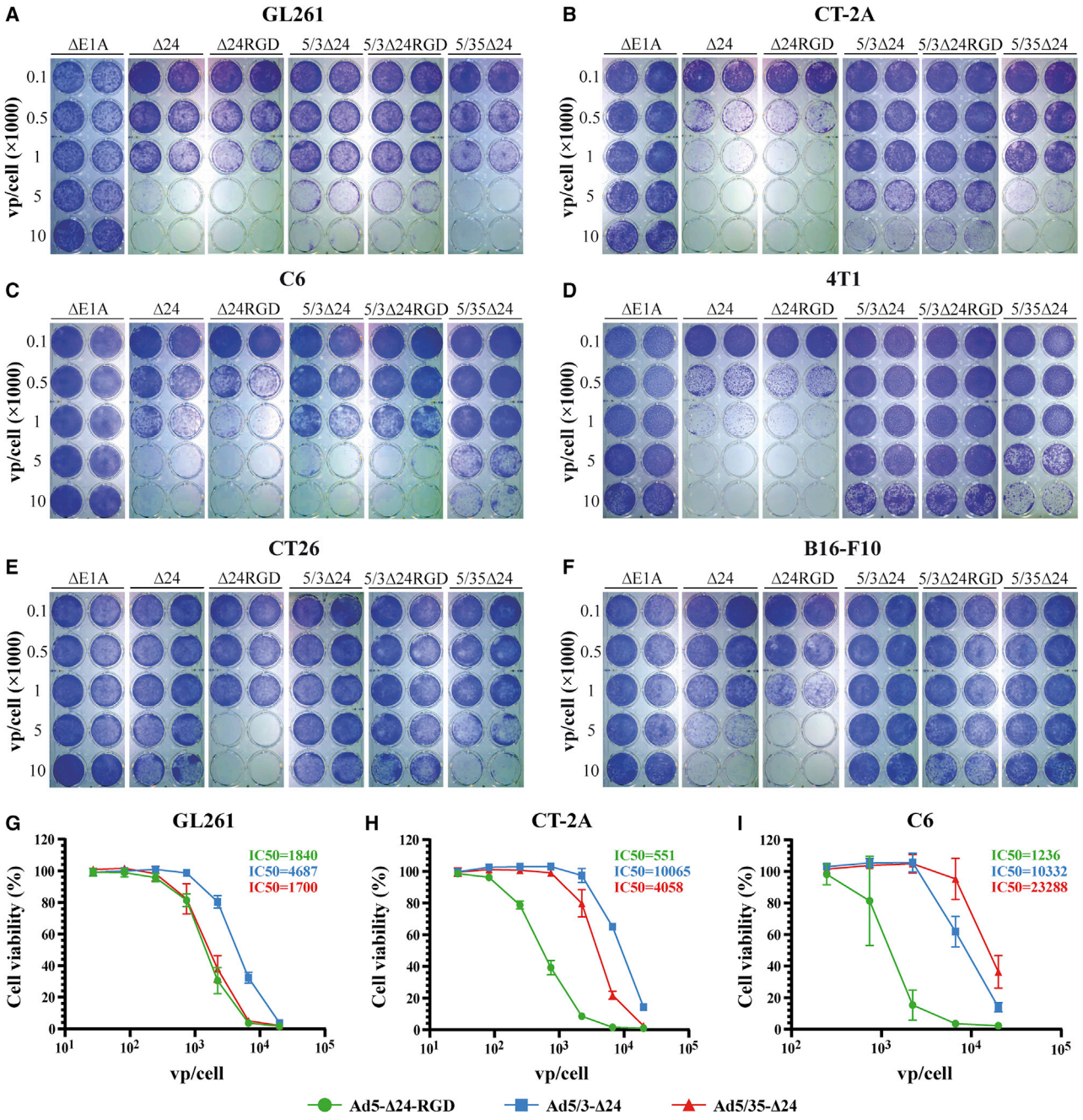

Figure 5. The comparative cytotoxic efficacy of the fiber-modified replication-competent recombinant adenoviruses in rodent glioma and carcinoma cell lines

(A–F) Crystal violet cell viability assays of rAd-infected cells 5 days post-infection. Cells (2.5×10^4/well) were infected in suspension with a serial dilution of the indicated rAds. Replication-defective Ad5ΔE1A was used as a negative control. Representative pictures of three independent experiments in technical duplicates with similar results are shown. (A) GL261 murine glioma cells. (B) CT-2A murine glioma cells. (C) C6 rat glioma cells. (D) 4T1 murine mammary carcinoma cells. (E) CT26 murine colon carcinoma cells. (F) B16-F10 murine melanoma cells. (G–I) Resazurin/Alamar Blue cell viability assays of rAd-infected cells 5 days post-infection. Cells (2.5×10^3/well) were infected in suspension with a serial 3-fold dilution of the indicated rAds starting from 20,000 vp/cell. Normalized data are presented as the mean ± SD of three independent experiments in technical triplicates. See also Figure S9.

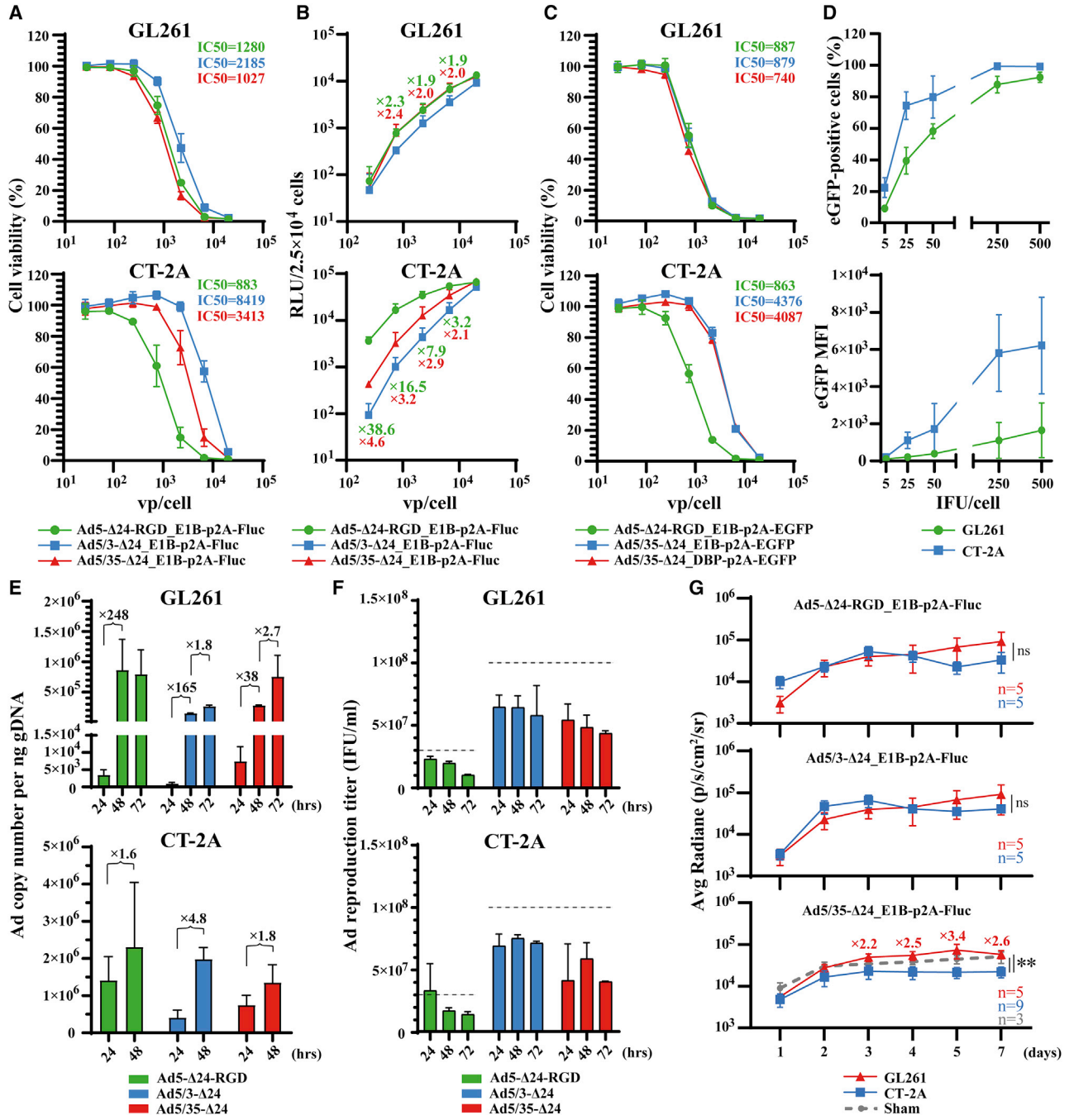

Figure 6. The comparative infectivity, replication, reproduction, and cytotoxic efficacy of the fiber-modified replication-competent recombinant adenoviruses in murine GL261 and CT-2A glioma cells

(A) Comparative dose-dependent cytotoxicity. Cells (2.5×10^3/well) were infected in suspension with a serial 3-fold dilution of the indicated luciferase-expressing rAds starting from 20,000 vp/cell and analyzed 5 days post-infection by resazurin/Alamar Blue cell viability assays. Normalized data are presented as the mean ± SD of two independent experiments in technical triplicates. (B) Comparative dose-dependent infectivity. Cells (2.5×10^4/well) were infected in suspension with a serial 3-fold dilution of the indicated luciferase-expressing rAds starting from 20,000 vp/cell. Luminescence (RLU) was analyzed 24 h post-infection. The mean ± SD of two independent experiments in four technical replicates is shown. Only ≥2-fold differences in the mean RLU values relative to Ad5/3-Δ24-RGD_E1B-p2A-Fluc are designated. (C) Comparative dose-dependent cytotoxicity. Cells (2.5×10^3/well) were infected in suspension with a serial 3-fold dilution of the indicated EGFP-expressing rAds starting from 20,000 vp/cell and analyzed 5 days post-infection by resazurin/Alamar Blue cell viability assays. Normalized data are presented as the mean ± SD of three independent experiments in technical triplicates. (D) Comparative dose-dependent infectivity. Cells (5×10^5/well) were infected in suspension with a serial dilution of Ad5/35-Δ24_DBP-p2A-EGFP and

(legend continued on next page)

survivors in an immune-competent syngeneic GL261 glioma model, while an immune costimulator GITRL-, OX40L-, or 4-1BBL-armed Ad5-Δ24-RGD significantly prolonged survival.[52–54] In these reports, a transgene expression cassette replaced the E3 locus, which is known to be responsible for immune evasion functions. To insert mOX40L by preserving the E3 locus (all viruses used in our study were non-E3 deleted), we tested two early loci (E1B and E2A/DBP) in the Ad genome. We first compared Ad5/35-Δ24_E1B-p2A-EGFP and Ad5/35-Δ24_DBP-p2A-EGFP in highly permissive A549 lung adenocarcinoma cells. Both viruses expressed EGFP but at significantly different levels, as shown by immunofluorescence (Figure 7A) and quantified by flow cytometry (Figure 7B). Both viruses formed plaques with similar efficiencies and sizes (both 3-[4,5-dimethylthiazol-2-yl]-2,5 diphenyl tetrazolium bromide [MTT]-stained and EGFP plaques), and no difference was observed compared with the parental Ad5/35-Δ24 (Figure 7C). The kinetics of cell death at low MOIs (0.02 and 0.2 IFU/cell) was similar between viruses (Figure 7D). The reproduction of viruses analyzed 24–72 h post-infection did not significantly differ (data not shown). Finally, the cytotoxicity of Ad5/35-Δ24_DBP-p2A-EGFP was comparable to that of the parental Ad5/35-Δ24 in a panel of cell lines (Figure 7E). Thus, although both tested viral loci may be suitable for the expression of a transgene fused via the p2A sequence (at least EGFP, since we were not able to rescue viruses with the DBP-p2A-Fluc fusion, as discussed above), the E2A/DBP locus supports higher transgene expression levels.

Long-term survival of mice bearing GL261 glioma following treatment with Ad5/35-Δ24_DBP-p2A-mOX40L

We constructed Ad5/35-Δ24_DBP-p2A-mOX40L-expressing mOX40L as a fusion with E2A/DBP via the p2A sequence. mOX40L expression was increased on the surface of infected human and murine glioma cells in a dose-dependent manner (Figure 8A). No significant difference was found between the mOX40L-expressing and parental viruses in the plaque assay on A549 cells 8 days post-infection (Figure 8B). We then compared the antitumor effect of Ad5/35-Δ24_DBP-p2A-mOX40L and the parental Ad5/35-Δ24 in mice bearing intracranial GL261 gliomas. Treatment with these rAds resulted in no increase in median survival (buffer = 31 days versus Ad5/35-Δ24 = 29 days and versus Ad5/35-Δ24_DBP-p2A-mOX40L = 31 days; $p = 0.8337$ and $p = 0.3574$, respectively) but led to 20% long-term survival for the Ad5/35-Δ24 treatment group and 33% for the Ad5/35-Δ24_DBP-p2A-mOX40L treatment group (Figure 8C). In a rechallenge experiment, the same tumor cells were inoculated in the contralateral hemisphere to determine whether the rAd-treated mice developed antiglioma immune memory (Figure 8D). All naive mice from the control group died of glioma within 35 days. In contrast, one out of two long-term survivor mice (50%) from the Ad5/35-Δ24 treatment group ($p = 0.2863$ versus control) and all three long-term survivor mice (100%) from the Ad5/35-Δ24_DBP-p2A-mOX40L treatment group ($p = 0.0066$ versus control) survived after tumor rechallenge (>80 days). These data indicate that the Ad5/35-Δ24_DBP-p2A-mOX40L-treated mice efficiently generated immunological memory against tumor cells in the GL261 glioma model.

DISCUSSION

Replication-competent Ad5-Δ24-RGD with the integrin-targeting RGD-4C peptide inserted into the HI loop of the fiber knob domain is currently the most clinically advanced rAd for glioma therapy.[4,5] Insertion of the RGD-4C peptide into the HI loop is known to significantly enhance the transduction of CAR-negative/low cells. Nevertheless, the transduction and cytolytic efficacy of fiber chimeric Ad5/3 were superior to those of Ad5RGD in different cancer cell types, including prostate cell lines,[55] melanoma cell lines,[37] breast carcinoma cell lines, short-term cultures, tissue slices,[38] clear cell carcinoma kidney cell lines,[39] gastric carcinoma tissue slices,[40] esophageal carcinoma cell lines,[41] bladder carcinoma cell lines,[42] and glioma cell lines and tissue slices.[43] Similarly, the transduction efficacy of Ad5/35 reporter virus was higher than that of Ad5RGD in melanoma cell lines and short-term cultures,[44] in sarcoma cell lines and short-term cultures,[45] and in glioma cell lines (n = 4) and short-term primary cultures (n = 2).[46] In the latter study, Ad5/35 transduced primary glioma cells even more efficiently than Ad5/3, and to the best of our knowledge, this is the only study evaluating the transduction efficacy of the fiber-modified replication-deficient Ad5RGD, Ad5/3, and Ad5/35 reporter viruses side by side in short-term glioma cultures, although the sample size was small. In this study, we evaluated the comparative infectivity and cytolytic efficacy of the replication-competent fiber-modified rAds and found that both Ad5/35-Δ24 and Ad5/3-Δ24 were generally more effective than Ad5-Δ24-RGD in human glioma cell lines (n = 4) and short-term cultures derived from primary brain tumors (n = 9).

Previously, Matsui et al. failed to rescue rAd with the RGD-4C peptide fused to the C terminus of the chimeric 5/35 fiber.[51] Although we succeeded in amplifying Ad5/35-Δ24-RGD to a high titer ($\approx 1.6 \times 10^{12}$ vp/mL from five T175 cm^2 flasks), it was severely defective compared with the parental Ad5/35-Δ24 in all of the tested cell lines. We also found that replication-competent Ad5/3-Δ24-RGD with the RGD-4C peptide at the C terminus of the chimeric 5/3 fiber showed similar or inferior cytotoxic efficacy depending on the cell line compared with the parental Ad5/3-Δ24 in human and rodent cells (n = 11). In contrast, Tyler et al. reported that in a panel of glioma cell lines

analyzed 24 h post-infection by flow cytometry. The mean percentage (%) ± SD and median fluorescence intensity (MFI) ± SD of EGFP-positive cells from two independent experiments are shown. (E) Ad DNA copy number quantification by qPCR. Cells (5×10^5/well) were infected in suspension at 2,000 vp/cell and collected 24, 48, and 72 h post-infection. Normalized data are shown as the mean ± SD of two independent experiments. qPCR runs were conducted in technical triplicates. (F) Total virus production (both culture cell extracts and supernatants including viral inoculum) was determined 24, 48, and 72 h post-infection using anti-Ad staining. Cells (5×10^5/well) were infected in suspension at an MOI of 60 IFU/cell (Ad5-Δ24-RGD) or 200 IFU/cell. The mean ± SD of two independent experiments is shown. The dashed lines indicate the total initial viral input. (G) C57BL/6 mice bearing CT-2A and GL261 tumors ($n \geq 5$ tumors per group) were injected intratumorally with the indicated rAds at a dose of 5×10^9 vp (5 μL), and tumor luminescence was measured at the indicated days post-treatment. $^{**}p \leq 0.01$ versus other groups, two-way ANOVA with Tukey's post hoc test. See also Figure S10.

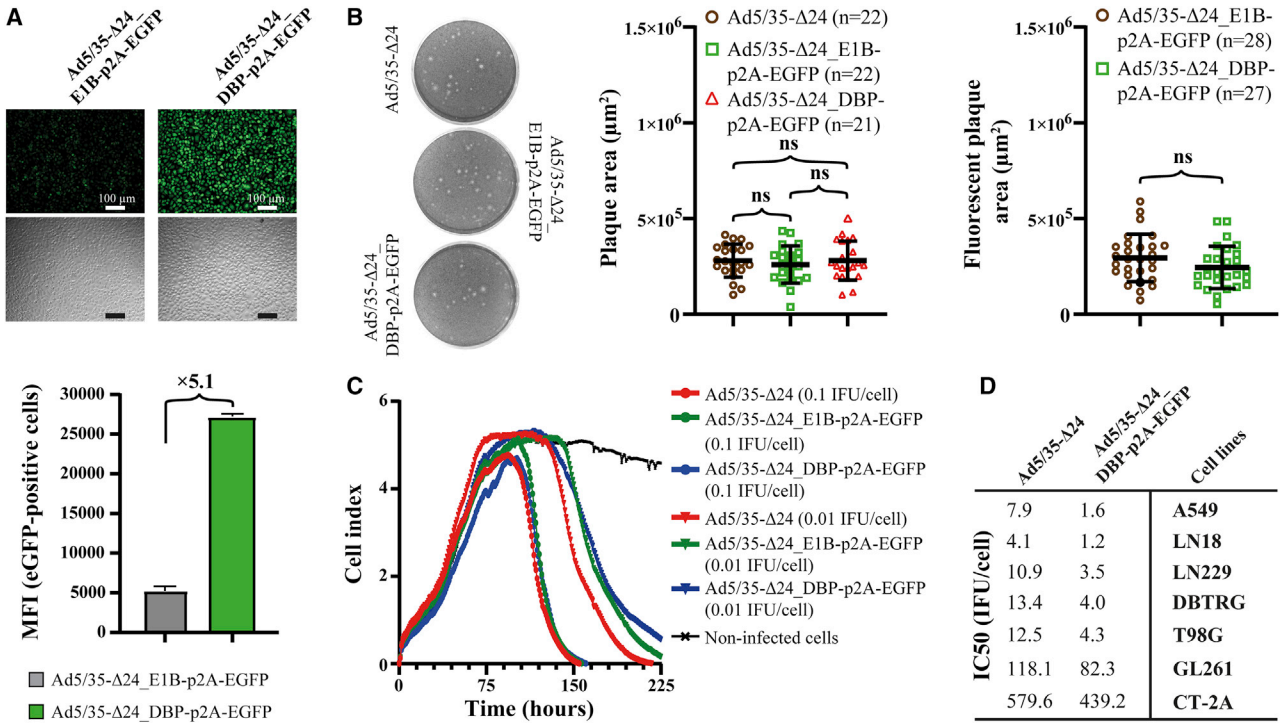

Figure 7. Characterization of Ad5/35-Δ24_E1B-p2A-EGFP and Ad5/35-Δ24_DBP-p2A-EGFP in A549 lung adenocarcinoma cells

(A) The Ad DBP locus supports a higher expression level of EGFP. Cells (5×10^5/well) were infected in suspension at an MOI of 50 IFU/cell, photographed with a fluorescence microscope 24 h post-infection (scale bars, 100 μm), and analyzed by flow cytometry. The mean ± SD of the MFI of EGFP-positive cells from two independent experiments is shown. (B) Comparison of the plaque areas of the indicated rAds in A549 cells at day 6 post-infection (1% agarose overlay) based on MTT staining or EGFP fluorescence. Data are presented as the mean ± SD; ns, nonsignificant difference by unpaired two-tailed t test with Welch's correction. The sample sizes are indicated in the figure. (C) Cell cytotoxicity kinetics analyzed by xCELLigence cell adhesion assay. A549 cells (2.5×10^3 cells/well) were infected in suspension with the indicated rAds (three technical replicates per dilution). Cell adhesion was monitored for a period of 225 h using the xCELLigence real-time cell analysis (RTCA) system. Impedance in electron flow (resistance to an alternating current) is plotted as arbitrary units called the cell index. (D) Table containing the IC50 values derived from resazurin/Alamar Blue cell viability assays in different cancer cell lines (two independent experiments). Human (5×10^3/well) and mouse (2.5×10^3/well) cells were infected in suspension with a serial 3-fold dilution of the indicated rAds starting from 100 IFU/cell and 2,000 IFU/cell, respectively, and analyzed 5 or 7 (T98G cells) days post-infection.

(n = 7), the replication-defective Ad5/3RGD reporter virus with the RGD-4C peptide fused to the C terminus of the chimeric fiber had enhanced transduction efficacy in the majority of the tested cell lines compared with the parental Ad5/3.[47] However, the replication-defective Ad5/3RGD reporter virus had comparable transduction efficiency with the parental Ad5/3 in a panel of carcinoma cell lines (n = 8).[42] Finally, in an independent study in a panel of glioma and carcinoma cell lines (n = 14), replication-competent Ad5/3-Δ24-RGD with the RGD-4C peptide placed at the C terminus of the chimeric fiber showed improved oncolytic potency over the parental Ad5/3-Δ24 in the majority of the tested cell lines.[48] Currently, we have no specific explanation for the inconsistency between the studies regarding the transduction/oncolytic efficiency of Ad5/3RGD-based viruses. However, taking into account our results and previous reports on fusing the RGD-4C peptide to the C termini of the fiber chimeric Ad5/35,[51] Ad5/11p,[56] and Ad5/41[57] with no additional enhancement in infectivity, we conclude that the C terminus of the chimeric fibers in general might not be a favorable location for the insertion of this targeting ligand.

It is believed that rAds based on Ad5 with the delta-24 modification effectively replicate only in cancer cells with disrupted pRb/E2F complex regulation but not in normal cells (quiescent or G1-arrested or even proliferating) with intact pRb due to the inability of the mutant E1AΔ24 protein to bind to pRb. In the original studies, Ad5-Δ24 did not efficiently replicate in lung fibroblasts arrested in the G_1 phase[10] and in normal microvascular endothelial cells and small airway epithelial cells arrested in the G_1 phase.[11] The replication of Ad5-Δ24 in proliferating normal cells was much more efficient than that in G_1-arrested cells, although it was still several orders of magnitude less than that in cancer cells.[11] However, these original reports describing the benefits of the delta-24 modification were contradicted by follow-up research.[12–17] Independent of the cellular proliferation status, both Ad5-Δ24 and a control virus with wild-type E1A caused cytotoxicity in a comparable manner in primary hepatocytes and lung and prostate epithelial cells.[16] Upon infection of human primary keratinocytes at an MOI of 1 PFU, Ad5-Δ24 was as cytotoxic as a control Ad with wild-type E1A.[14] The viral yield at day 5 after infection with Ad5-Δ24-RGD was not reduced compared with that of Ad5RGD

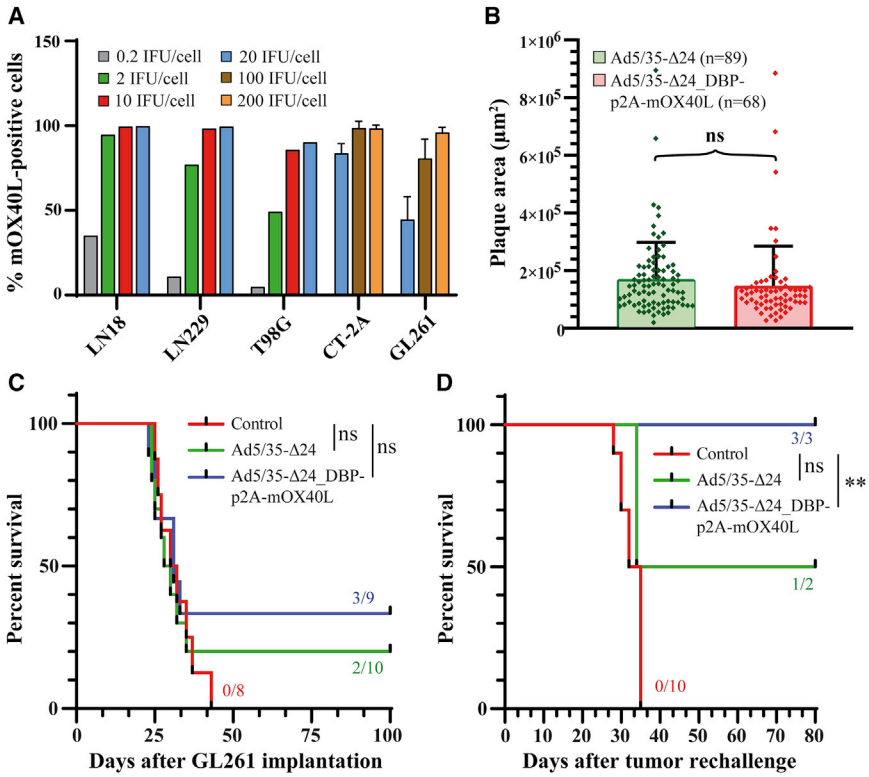

Figure 8. Ad5/35-Δ24_DBP-p2A-mOX40L treatment produces long-term survivors with immunological memory in an orthotopic syngeneic GL261 glioma model

(A) Dose-dependent mOX40L expression in human (n = 1) and murine glioma cells (n = 3 independent experiments) infected with Ad5/35-Δ24_DBP-p2A-mOX40L at the indicated MOIs and analyzed by flow cytometry 24 h post-infection. (B) Comparison of the plaque areas of the indicated rAds in A549 cells at day 8 post-infection. Data are presented as the mean ± SD; ns, nonsignificant difference by unpaired two-tailed t test with Welch's correction. The sample sizes are indicated in the figure. (C) Kaplan-Meier survival curves of mice bearing GL261 tumors. rAds were intratumorally injected (1×10^8 IFU; 5 μL) on days 7, 9, and 11 after tumor cell implantation (n = 10, Ad5/35-Δ24; n = 9, Ad5/35-Δ24_DBP-p2A-mOX40L; n = 8, Ad storage buffer). Several long-term survivors (>100 days) in the rAd-treated groups are shown. Log rank test: Ad5/35-Δ24 versus Ad buffer, p = 0.8337; Ad5/35-Δ24_DBP-p2A-mOX40L versus Ad buffer, p = 0.3574). (D) GL261 rechallenge experiment with tumor cells implanted into the contralateral hemisphere of the long-term survivors (n = 2, Ad5/35-Δ24; n = 3, Ad5/35-Δ24_DBP-p2A-mOX40L) and naive mice (n = 10). Log rank test: Ad5/35-Δ24 versus Ad buffer, p = 0.2863; Ad5/35-Δ24_DBP-p2A-mOX40L versus Ad buffer, p = 0.0066).

with wild-type E1A in normal fibroblasts and HUVECs infected at MOIs of 25 and 3, respectively.[13] Growth-arrested HUVECs and MRC9 cells infected with Ad5-Δ24 at MOIs of 20, 1, or 0.01–100 PFU showed a robust induction of the S phase, supported effective virus reproduction, and exhibited a similar decrease in viability compared with the cells infected with a control Ad with wild-type E1A (of note, in both viruses, E1A was regulated by the cytomegalovirus [CMV] promoter).[12] Ad5-Δ24-RGD efficiently killed human primary mesothelial cells at doses of $\leq$10 vp/cell in the crystal violet and 3-(4,5-dimethylthiazol-2-yl)-5-(3-carboxymethoxyphenyl)-2-(4-sulfophenyl)-2H-tetrazolium (MTS) cell viability assays.[15] In the crystal violet cell viability assay, Ad5-Δ24 and wild-type Ad5 were comparably toxic in primary human astrocytes at 1,000 and 100 vp/cell at day 5 post-infection, showing complete or nearly complete cell killing. At doses of 10 and 1 vp/cell, wild-type Ad5 was slightly more cytopathic than Ad5-Δ24.[17] We found that the relative cytotoxicity of the fiber-modified rAds with the delta-24 modification in primary normal proliferating cultures (HEFs, OECs, HA-VSMCs, HUVECs, and embryonic astrocytes) was cell type-dependent, with Ad5/35-Δ24 and Ad5/3-Δ24 exhibiting generally more cytopathic effects in a tested range of doses (100–0.01 vp/cell). Importantly, our *de novo*-generated delta-24- and fiber-modified rAds killed both proliferating primary normal cells and short-term primary glioma cultures with similar efficiencies and kinetics (IC50 values). Moreover, the delta-24- and fiber-modified rAds used in this study killed embryonic fibroblasts and astrocytes with comparable efficiencies to the delta-24-nonmodified counterpart rAds reported previously.[58,43] Taken together, these data indicate that the delta-24 modification alone does not confer significant replication selectivity. This finding raises safety concerns regarding possible damage to normal cells near tumor tissue during intratumoral rAd administration. Additional tumor-specific regulations (e.g., by promoters or miRNAs) to improve the safety of fiber chimeric adenoviral therapy might be required. However, most adult brain cells are quiescent, and the tissue context might be very important in the severity of rAd cytotoxicity. In support of this assumption, the amounts of progeny virus produced after 7 days in normal human brain tissue *ex vivo* infected with wild-type Ad5 and Ad5-Δ24 at an MOI of 10^8 PFU/tissue piece were similar but very low (below 10^4 PFU).[59] Furthermore, in a phase I trial of Ad5-Δ24-RGD in recurrent glioma patients receiving a single intratumoral viral dose (1×10^7–3×10^{10} vp), no dose-limiting toxicities and no maximum tolerated dose were identified.[6] Finally, E1A critically influences cytoplasmic interferon signaling pathways and dampens the innate cellular response to infection by inhibiting the expression of immunologically active host genes.[60] It is possible that the *E1A*Δ24 mutation induces loss of function(s) that is less notable in *in vitro* testing but is remarkable *in vivo*. Due to the relatively enhanced cytotoxicity in normal proliferating cell cultures, additional safety improvements in the fiber chimeric Ad5/3 and Ad5/35 might be required, although it is certainly difficult to speculate about such a need until considerable toxicity has been established in a relevant permissive *in vivo* model or in clinical trials.

We found that CAR expression varied from a low to high levels in established cell lines, while it was barely detectable in short-term glioma cultures. The expression of CAR in glioma tissues and short-term primary glioma cultures was frequently barely detectable.[19–22,25] However, in established glioma cell lines and in mouse xenografts of short-term glioma cultures, CAR expression was found to be upregulated compared with that of their parental tumors.[21] A similar and seemingly contradictory situation with the expression of CAR was also reported for melanoma. Melanoma tissue cells or freshly isolated tumor cells expressed negligible CAR, while CAR expression was upregulated in melanoma cells after prolonged passaging,[58] indicating that the expression of CAR by tumor cells *in vitro* or *in vivo* as xenografts can be an artifact.[21,58] We also found that DSG2 expression varied from low to high levels in established cell lines, while it was largely undetectable in the majority of the tested short-term cultures. In support, Niittykoski et al. observed that short-term glioma cell cultures significantly reduced or lost DSG2 but not CD46 expression during passaging compared with their parental tumor tissues.[19] Finally, we found that CD46 was expressed abundantly in all of the tested human cell cultures, consistent with previous reports.[19,20] Altogether, these data imply that for personalized oncolytic virotherapy, if applicable at all, measuring the expression levels of adenoviral receptors perioperatively should be preferable and more relevant from a practical point of view, although the expression levels of CAR, DSG2, and CD46 and integrins αVβ3/αVβ5 did not predict, at least *in vitro*, the relative oncolytic efficiency of the fiber-modified rAds tested in our study. Our findings are consistent with previous reports. In some studies, CAR expression directly correlated with the level of Ad5 cell-surface binding or transduction, while no such correlation was observed with the expression levels of αvβ3/αvβ5 integrins.[21,61,62] In contrast, others reported no correlation between CAR expression levels and Ad5 transduction.[22–24] In cells expressing low to barely detectable CAR, binding to the integrin αVβ5 was sufficient for both Ad5 attachment and internalization,[23] and low-passage glioma cells with barely detectable CAR levels could be transduced with Ad5.[22] Moreover, there was no correlation between the transduction efficiency of Ad5/35 reporter virus and the expression levels of CD46 in a panel of pancreatic and breast cancer cell lines,[63] in esophageal and oral carcinoma cells,[64] in colorectal carcinoma cells,[65] and in normal human B lymphocytes and cell lines of lymphoid origin.[66] In the latter study, it was revealed that the transduction efficiency of Ad5/35 depended largely on the cell-specific intracellular trafficking routes.

We revealed that both CT-2A and GL261 murine glioma cells were susceptible to Ad5/35-Δ24 and Ad5/3-Δ24 infection. Moreover, Ad5/35-Δ24-based rAds were as cytotoxic as Ad5-Δ24-RGD-based rAds in GL261 cells. We also found that the most abundantly expressed early Ad locus E2A/DBP[67] may support efficient transgene expression (at least, EGFP and mOX40L) when it is fused via a p2A sequence. Finally, our data on long-term survivor mice (33%) cured of orthotopic syngeneic GL261 gliomas after treatment with Ad5/35-Δ24_DBP-p2A-mOX40L are consistent with the survival rates reported for Ad5-Δ24-RGD expressing the immune costimulator mCD137L (4-1BBL)[52] or mOX40L[53] under the CMV promoter from the E3 region in the GL261 glioma model (23% and 20% long-term survival, respectively). In these and other reports, coadministration of rAd expressing an immune costimulator with antibodies to PD-L1 further increased the percentage of long-term survivors with efficient immunological memory on tumor rechallenge, indicating that a combinatorial approach in immunovirotherapy is a vital strategy for treating deadly gliomas. We believe that our study will pave the way for further development of potent fiber chimeric Ad5/35-based viruses for brain malignancies.

MATERIALS AND METHODS

Cell lines

Human embryonic kidney HEK293, lung adenocarcinoma A549, gliomas U118, T98G, DBTRG, LN18, and LN229, rat glioma C6, murine B16-F10 melanoma (ATCC), 911, murine glioma CT-2A (SCC194, Sigma), and GL261 cells (DSMZ Cell Culture Collection) were grown in DMEM GlutaMax (Gibco) containing 10% FBS (HyClone). Murine mammary 4T1 carcinoma cells and colon CT26 carcinoma cells (ATCC) were cultured in RPMI-1640 (Gibco) supplemented with glucose (4.5 g/L), L-glutamine (2 mM), sodium pyruvate (1 mM), HEPES (10 mM), and 10% FBS. Primary human embryonic dermal fibroblasts and embryonic astrocytes (a cell bank of V.P. Serbsky National Medical Research Center, Moscow, Russia), and primary OECs[68] were cultured in DMEM/F12 (Gibco) with 10% FBS. T/G HA-VSMCs (CRL-1999, ATCC) were cultured in F-12K medium (Gibco) with 2 mM L-glutamine; 1,500 mg/L sodium bicarbonate; 0.05 mg/mL ascorbic acid (Sigma); 0.01 mg/mL insulin (Gibco); 0.01 mg/mL transferrin (Gibco); 10 ng/mL sodium selenite (Gibco); 0.03 mg/mL endothelial cell growth supplement (ECGS, Sigma); HEPES (10 mM); TES (10 mM, Sigma); 10% FBS; and 25 μg/mL amphotericin B (Gibco). Primary HUVECs (a cell bank of V.P. Serbsky National Medical Research Center) were cultured in F-12K medium with 2 mM L-glutamine, 1,500 mg/L sodium bicarbonate, 0.03 mg/mL ECGS, 10% FBS, and 25 μg/mL amphotericin B. Glioma (III–IV grade) and medulloblastoma short-term cell cultures (passages 5–10 used for cytotoxicity assays and flow cytometry) were established and cultured as described in the Supplemental materials and methods. The culture media were supplemented with 100 U/mL penicillin and 100 μg/mL streptomycin. All of the cell lines were maintained in an incubator at 37°C in a humidified atmosphere of 95% air and 5% CO_2 and were tested for mycoplasma contamination. All human cancer cell lines were authenticated by short tandem repeat (STR) analysis in 2019.

Construction of rAds

We first assembled a cloning vector, pSC101-CmR-PacI, containing the pSC101 low copy origin of replication with the partition (par) locus (derived from pSC101-Timer plasmid, Addgene #103057), chloramphenicol resistance gene, and two PacI sites for releasing the adenoviral genome. The full-length genome of human adenovirus 5 (strain Adenoid 75, VR-5, ATCC) was incorporated into this cloning vector, as described previously,[69] using RecET-mediated linear-linear homologous recombination in the *Escherichia coli* GB05-dir strain

(Gene Bridges, Heidelberg, Germany). For modification of the adenoviral genome, a selection/counterselection *rpsL*-neo cassette (from the "Counter-Selection BAC Modification Kit," Gene Bridges) and λ-Red-mediated linear-circular homologous recombination in the *E. coli* GB08-red strain (Gene Bridges) were exploited according to the flowchart in Figure S11. For recombination, 30 μL of overnight culture was inoculated into 1.4 mL of low-salt lysogeny broth (LB; 5 g/L NaCl) containing streptomycin (linear-linear homologous recombination) or chloramphenicol (linear-circular homologous recombination to maintain a plasmid) and grown in 1.5 mL tubes with needle-punctured caps at 950 RPM and 37°C in a thermoshaker TS-100C (BioSan, Latvia). At an absorbance of ≈0.4, 50 μL of 10% L-arabinose was added (final 0.35% w/v) to induce *RecET* or *redγβα*/*recA* expression in *E. coli* GB05-dir and *E. coli* GB08-red strains, respectively. After 35 min (absorbance ≈0.7–0.8), cells were harvested by centrifugation at 5,900 × *g* at room temperature (all procedures afterward were carried out at room temperature irrespective of the type of recombination), washed twice with autoclaved ddH_2O and once with 10% (v/v) glycerol, and resuspended in a final volume of 30–35 μL in 10% glycerol. For linear-linear homologous recombination, adenoviral genomic DNA (≈500 ng) and the linearized cloning vector (≈500 ng) with homologous arms were added to the cells, mixed and transferred to an electroporation cuvette with a 0.1 cm gap (Bio-Rad), and electroporation was carried out with a MicroPulser (Bio-Rad) at a constant voltage of 1.7 kV (Ec1 program). For linear-circular homologous recombinations, the pSC101-CmR-Ad5 vector was maintained inside the cells by chloramphenicol selection, and only the PCR product, annealed complementary oligonucleotides (oligos), or single-strand oligos (≈500 ng) were added for electroporation. The cells were immediately removed from a cuvette by mixing with 1 mL of prewarmed low-salt LB medium and then were incubated in a thermoshaker at 37°C and 950 RPM for 1.5 h. The cells were collected by centrifugation at 5,900 × *g* and usually all plated on low-salt LB agar containing the appropriate antibiotics. Sometimes, a $1/10^{th}$–$1/100^{th}$ part of the cells was sufficient to plate to prevent extensive colony background/formation of a bacterial lawn. Antibiotics were used at the following final concentrations in LB and solid media: chloramphenicol (15 μg/mL), kanamycin (30 μg/mL), and streptomycin (200 μg/mL). A routine diagnostic restriction digest of rAds after each round of recombination was carried out using EcoRV and XhoI (Thermo Scientific). Screening of clones was conducted using PCR followed by sequencing. All the oligonucleotides (Table S4) were ordered from Evrogen (Moscow, Russia) or Syntol (Moscow, Russia) as unpurified (for screening colony PCR or sequencing) or high-performance liquid chromatography (HPLC)/PAGE-purified (for recombination) depending on the length of oligo. For *in silico* linear-linear and linear-circular homologous recombination, Molecular Cloning Designer Simulator (MCDS) software was used.[70]

DNA amplification and gel extraction

For amplification of DNA fragments for recombination, Phusion Green Hot Start II High-Fidelity PCR Master Mix (Thermo Scientific) was used according to the manufacturer's recommendations. The predicted annealing temperatures for each oligo pair were determined using an online T_m Calculator (Thermo Scientific). With the QIAquick Gel Extraction Kit (Qiagen, Germany), PCR fragments were isolated from 0.8% agarose stained with SYBR Safe DNA Gel Stain (Invitrogen) and were visualized with Safe Imager 2.0 Blue-Light Transilluminator (Invitrogen). Before electroporation, gel-extracted PCR products were desalted using membrane filters (#VSWP02500, Millipore). For colony PCR screening, DreamTaq Green PCR Master Mix (Thermo Scientific) or PCR ScreenMix (Evrogen) was used. Purified genomic DNA of human adenovirus 3 (strain G.B., VR-847, ATCC) and adenovirus 35 (strain Holden, VR-718, ATCC) were used as templates for constructing the fiber chimeric Ad5/3 and Ad5/35.

Transfection, adenovirus amplification, purification, storage, and titering

HEK293 cells were seeded onto 3 cm plates (two for each virus rescue) and transfected at 70%–90% confluency with the PacI-linearized rAd genome (2.5 μg/plate as measured by gel densitometry) purified with ethanol plus glycogen precipitation using 5 μL of reagent P3000 and 5 μL of Lipofectamine 3000 (Invitrogen). After 3–5 days, both cells and supernatant were collected, freeze-thawed three times, and centrifuged at 2,000 × *g* for 5 min, and all supernatant was added to one near-confluent T75 flask with A549 cells. Replication-deficient Ad5Δ*E1A* was amplified in 911 cells. Depending on the rAd and the efficiency of transfection, we usually observed signs of cytopathic effects after 3–10 days. When at least half of the cells were rounded, both cells and supernatant were collected, freeze-thawed three times, and centrifuged at 2,000 × g for 10 min, and $1/8^{th}$–$1/10^{th}$ part was diluted and added to five near-confluent T175 flasks. The infected cells were collected within 2–3 days. After three cycles of freeze-thawing and clearing by centrifugation at 2,000 × *g* for 10 min, the cell lysate solution (≈5 mL of a rescued virus in DMEM without serum) was transferred on top of a CsCl step gradient (5 mL of 1.27 g/cm^3 and 3 mL of 1.41 g/cm^3 ρCsCl in 20 mM HEPES, 150 mM NaCl buffer, pH 7.6) in 14 mL Beckman ultraclear tubes (#344060). The ultracentrifugation tubes were filled to the top with HEPES buffer and centrifuged in a Beckman SW40Ti rotor at 28,000 RPM (100,000 × *g*) in a Beckman Avanti 90L ultracentrifuge at 8°C for 1 h without the brake. Two rounds of ultracentrifugation were conducted. The virus bands were collected in a volume of ≈500 μL and dialyzed in Slide-A-Lyzer 10 K dialysis cassettes (Thermo Scientific) against 1 L of storage buffer (5 mM Tris, 75 mM NaCl, 1 mM $MgCl_2$, 5% sucrose [w/v], 0.005% PS-80, pH 8.0) at 4°C for 2 h and then overnight. The viruses were aliquoted and stored at −70°C. The viral genomic integrity and the presence of correct modifications in purified rAds were confirmed by restriction digests and sequencing.

Since rAds with the RGD-4C peptide inserted into the HI loop of the fiber knob domain tend to macroscopically and/or microscopically aggregate during CsCl gradient ultracentrifugation,[71,72] they were purified by a 2 × iodixanol discontinuous density gradient according to the protocol.[73] For Beckman ultraclear 14 mL tubes, we used the following volumes of step gradients: Sol 4 (15%, 1.5 mL), Sol 3

(25%, 3 mL), Sol 2 (40%, 3 mL), and Sol 1 (54%, 0.5 mL). Ultracentrifugation was conducted at 35,000 RPM (155,000 × *g*) in an SW40 Ti rotor at 8°C for 1 h. After the second round of ultracentrifugation, iodixanol from the purified virus/iodixanol fraction was first removed by size-exclusion column chromatography using virus storage buffer and Zeba spin desalting column, 7K MWCO, 2 mL (Thermo Scientific), and then the remaining trace amounts were removed by overnight dialysis against 1 L of Ad storage buffer, as described above. For confirmation of the absence of aggregation, the particle size distribution (polydispersity index [PDI]) was measured using a Zetasizer Nano ZS (Malvern Instruments, UK). Measurements were carried out at a concentration of 3×10^{10} vp/mL in autoclaved deionized water in cuvettes at 25°C with the default instrument settings and automatic analysis.

The physical titer (optical particle units [OPU]) was determined by measuring the absorbance at 260 nm in the range of 0.1–1.0 optical density (OD) on an NP80 spectrophotometer (Implen, Germany) using at least three dilutions. DNA was released from virions in lysis buffer (100 mM Tris, 10 mM EDTA, 0.1% SDS) in a thermoshaker at 56°C and 500 RPM for 10 min. OPU for rAds were calculated using the following formula: OPU/mL = (absorbance at 260 nm) × (dilution factor) × (1.1×10^{12}). For determination of the titer of IFU, rAds were titered on A549 cells or 911 cells (Ad5Δ*E1A*) by the Adeno-X Rapid Titer Kit (TaKaRa Bio, USA) according to the manufacturer's instructions. Briefly, cells (1.25×10^5 cells/well in 48-well plates) were infected with serial dilutions of the viral stocks. Two days later, cultures were fixed with 100% ice-cold methanol for 10 min at −20°C and stained for hexon expression. Hexon-stained areas were counted under a light microscope (10× objective) in 10 random fields/well. The viral titer was calculated using the following formula: IFU/mL = [(average positive cells/field) × (fields/well)]/[volume virus (mL) × dilution factor]. The vp (or OPU) to IFU ratios for preparations of rAds are listed in Table S1.

Extraction of viral genomic DNA

The CsCl- or iodixanol-purified viral particles were hydrolyzed by adding SDS (final 0.5% v/w) and proteinase K (0.5 mg/mL) to buffer (10 mM Tris-HCl, pH 8.0, 1 mM EDTA, #17890, ThermoScientific) and by incubation at 56°C for 2 h with low-speed shaking (300 RPM). Then, viral genomic DNA was extracted using phenol:chloroform:isoamyl alcohol mixture (25:24:1) according to the manufacturer's instructions (#77617, Sigma). To isolate 2–20 μg of adenoviral genomic DNA, it is necessary to add 5–50 × 10^{10} vp of Ad with a 36 kb genome size [number of copies = (amount in ng*6.022 × 1,023)/(length in bp*1 × 109*650)].

Crystal violet cell viability assay

The cells were seeded in a 24-well plate (2.5×10^4/well, 0.4 mL of medium with 10% FBS) and infected in suspension (50–100 μL of viral inoculum) with serial dilutions of rAds (vp/cell, designated in figures, two wells/dilution). Several days post-infection, additional complete growth medium was added to each well. Five days (murine cells) or 8 days (human cells) post-infection, the wells were washed once with PBS, fixed in methanol for 10 min at −20°C, stained with crystal violet (0.05% in aqueous 20% methanol) for 30 min, washed with distilled water, dried, and scanned with an Epson Perfection V370 scanner.

Resazurin/Alamar blue cell viability assay

The cells (5,000 cells/well for human cells and 2,500 cells/well for rodent cells) were seeded in 96-well plates (80 μL of medium with 10% FBS) and infected in suspension (20 μL of viral inoculum) with serial dilutions of rAds (vp/cell or IFU/cell, designated in figures). The next day, 100 μL of additional complete medium was added to each well. At the indicated days of analysis, 100 μL of complete medium with 10% resazurin/Alamar Blue reagent was added to each well. A 0.15 mg/mL solution of resazurin (sodium salt, pure, certified, #418900010, Acros Organics, China) in PBS was used (stored frozen and aliquoted for single use). After 4 h of incubation, fluorescence was measured in a PerkinElmer EnSpire multimode plate reader with set excitation and emission wavelengths of 560 and 590 nm, respectively.

In vitro bioluminescent assays

The cells (2.5×10^4 cells/well) were seeded onto 96-well plates (80 μL of complete culture medium) and infected in suspension (20 μL of viral inoculum) with serial dilutions of rAds. Twenty-four hours later, D-Luciferin (30 mg/mL in PBS, ab143655, Abcam) was diluted 1:200 in complete culture medium (150 μg/mL final concentration) and added (100 μL) to the cells 10 min before imaging. Luminescence (RLU) was measured in a PerkinElmer EnSpire multimode plate reader.

Adenovirus replication

The cells (5×10^5/well of a 12-well plate) were infected in suspension (total 1 mL) with rAds at a dose of 100 vp/cell for human or 2,000 vp/cell for murine cell lines. The monolayers were washed twice with PBS 24–72 h post-infection, and the cells were trypsinized and pelleted in a microcentrifuge. Total DNA was purified by an ExtractDNA Blood & Cells kit (#BC111M, Evrogen, Russia) according to the manufacturer's instructions. qPCRmix-HS (UDG) (#PK245L, Evrogen) with TaqMan probes and PowerSYBR Green PCR Master Mix (Applied Biosystems) were used for quantification of Ad DNA copy numbers in human and mouse samples, respectively. The final concentrations of primers and probes were 900 and 250 nM, respectively. Reaction conditions were according to the qPCR master mix manufacturer's recommendations. PCR runs were performed on a StepOnePlus Thermocycler (Applied Biosystems). For generation of standard curves and normalization, fragmented genomic DNA from the human Raji cell line (100 μg/mL, #NA102, Evrogen), genomic DNA from the murine 4T1 cell line, and viral genomic DNA extracted from CsCl-purified viral particles (concentrations determined by means of a Qubit 2.0 Fluorometer, Invitrogen) were exploited. The following primers, which were previously described,[74,75] were used: viral L2 forward, 5′-TTGTGGTTCTTGCAGATATGGC-3′, reverse, 5′-TCGGAATCCCGGCACC-3′; probe 5'-[FAM]-CTCACCTGCCG CCTCCGTTTCC-[RTQ1]-3' (efficient RTQ1 quencher for FAM was developed by Syntol, Russia); hB2M forward, 5′-CCAGCAGA GAATGGAAAGTCAA-3′, reverse, 5′-TCTCTCTCCATTCTTCAG

TAAGTCAACT-3′, probe, 5'-[FAM]-ATGTGTCTGGGTTTCATC CATCCGACA-[RTQ1]-3'; mB2M forward, 5′-ACAGTTCCACCC GCCTCACATT-3′, reverse, 5′-TAGAAAGACCAGTCCTTGCTGA AG-3′ (MP201317, OriGene). The efficiency of PCR runs was routinely ≥95%.

Adenovirus reproduction

Human cells (2.5×10^5 cells/well of a 24-well plate) and mouse cells (5×10^5 cells/well of a 12-well plate) were infected in suspension (total 0.5 or 1 mL, respectively) with rAds, and samples (both supernatant and cells) were collected at the indicated time points. After three cycles of freeze-thawing, the infectious titers were determined by immunocytochemistry on A549 cells 2 days post-infection using polyclonal anti-adenovirus type 5 antibody (1:2,500, ab6982, Abcam), goat anti-rabbit immunoglobulin G (IgG) H&L (horseradish peroxidase [HRP]) (1:1,000, ab6721, Abcam), and DAB substrate kit (ab64238, Abcam) for visualization of positive cells.

Plaque assay

A549 monolayers seeded in 6-well plates were infected with serial dilutions of rAds. Two hours post-infection, the viral inoculum was removed, and the cells were covered with 2–3 mL of a mix of DMEM/5% FBS/1% agarose. Later, DMEM/5% FBS overlay was added. For evaluation of the plaque size, monolayers were stained by incubating with a $1/10^{th}$ volume of thiazolyl blue tetrazolium bromide (MTT, 0.5 mg/mL) at 37°C for 4 h. The plaques were photographed at 50× with a Leica DM3000 microscope and quantified with Leica Application Suite microscope software.

xCELLigence cell adhesion assay

A549 cells (2.5×10^3 cells/well) were plated in an E-plate 16 (ACEA Bio) with gold microelectrodes embedded within each well and were infected in suspension with rAds (3 technical replicates/dilution). Cell adhesion was monitored over time using the xCELLigence real-time cell analysis (RTCA) system instrument (ACEA Bio). Impedance in electron flow (resistance to an alternating current) is plotted as arbitrary units called the cell index.

Intracranial glioma modeling and treatment

The experimental procedures were performed in accordance with Directive 2010/63/EU of September, 22, 2010, and approved by the local ethical committee of V.P. Serbsky National Medical Research Center. The study was carried out in compliance with the ARRIVE guidelines. Eight-week-old female immune-competent C57BL/6 mice obtained from the Scientific Center of Biomedical Technologies of the Russian Academy of Science (Andreevka, Moscow, Russia) were maintained in individually ventilated cages (Tecniplast, Italy). Cells were anesthetized by intraperitoneal injection of 50 mg/kg zoletil with 5 mg/kg xylazine and intracranially implanted with 5×10^4 GL261 murine glioma cells in the right hemisphere using a stereotaxic instrument (Stoelting, USA) at stereotaxic coordinates of bregma, 2 mm lateral, 1 mm caudal, and 3 mm ventral. Five microliters of cell suspension in DMEM was delivered at a depth of 3 mm using a 100 μL Hamilton microsyringe and a 2 pt style needle at a rate of 0.5 μL/min. The microsyringe was removed at a rate of 0.5 mm/min. Mice were randomly allocated to groups (n = 10, Ad5/35-Δ24; n = 10, Ad5/35-Δ24_DBP-p2A-mOX40L; n = 8, control/Ad buffer). The sample sizes were determined according to standard practice in the field. At days 7, 9, and 11 after tumor cell implantation, mice were injected intratumorally with either 5 μL of virus storage buffer or 1×10^8 IFU of rAds. One animal from the Ad5/35-Δ24_DBP-p2A-mOX40L group was excluded from the study due to premature death before receiving all three injections of rAd. The person who administered treatments and monitored the survival over time was blinded to the allocation groups. Mice were euthanized when they demonstrated moribund behavior. At 100 days post-tumor implantation, the surviving animals were intracranially rechallenged with 5×10^4 GL261 murine glioma cells in the contralateral hemisphere and were monitored for >80 days.

For *in vivo* bioluminescence imaging, GL261 and CT-2A glioma modeling was performed as described above. Quantitative analysis of bioluminescence signals (radiance) was performed using an IVIS Spectrum system (PerkinElmer) on mice (n = 5, Ad5-Δ24-RGD_E1B-p2A-Fluc and Ad5/3-Δ24-RGD_E1B-p2A-Fluc; n = 5–9, Ad5/35-Δ24-RGD_E1B-p2A-Fluc) at days 1, 2, 3, 4, 5, and 7 after a single intratumoral stereotactic injection of rAds (5×10^9 vp in 5 μL of storage buffer). The injections of rAds were carried out 14 days after inoculation of 5×10^4 GL261 or CT-2A glioma cells. The animals received D-Luciferin potassium salt (#122799, PerkinElmer, or ab143655, Abcam) intraperitoneally at a dose of 3 mg/animal (≈20 g weight) 10–15 min before imaging. Heads of the mice were not shaved before imaging. IVIS parameters for imaging were exposure time: 30 s; binning: 8 (medium); f/stop (lens aperture): 1.

Flow cytometry

The cells were detached by treatment with Accutase (StemCell Technologies) and washed with flow cytometry buffer consisting of PBS supplemented with 2 mM EDTA and 1% BSA. At least 5×10^5 cells were stained with conjugated antibodies at concentrations recommended by the manufacturers in a total volume of 100 μL, incubated in tubes in a thermoshaker at a low rotation speed at 4°C for 1 h, washed once with buffer, and resuspended in buffer. Data were acquired employing a MoFlow XDP (Beckman Coulter) and analyzed using Summit V5.2 (Beckman Coulter). At least 1×10^4 events for established cell lines and 0.5×10^4 events for short-term cultures were analyzed. Antibody conjugates are as follows: CAR-FITC (clone 271, 10799-R271-F, Sino Biological, China); DSG2-AF488 (CSTEM28, 53-9159-80, eBioscience, USA); CD46-PE (MEM-258, SAB4700432, Milli-Mark/Sigma); CD46-APC/Cy7 (TRA-2-10, 352410, Biolegend, USA); integrin αV/β3-APC (23C6, 304416, Biolegend); integrin αV/β5-PE (P1F6, 920008, Biolegend); mCD40L(CD252)-APC (RM134L, 108,811, Biolegend), isotypes: IgG-FITC (11-4614-80, eBioscience); IgG2b-AF488 (eBMG2b, 53-4732-80, eBioscience); IgG1-APC (MOPC-21, 400122, Biolegend); IgG1-PE (MOPC-21, 400114, Biolegend); and IgG1-APC/Cy7 (MOPC-21, 400128, Biolegend).

Statistics

The data are expressed as the mean ± standard deviation (SD) or standard error of the mean (SEM), as indicated. The D'Agostino-Pearson and Shapiro-Wilk normality tests were performed. An unpaired two-tailed Student's t test with Welch's correction was used to evaluate the differences between groups in quantitative studies of cultured cells. The number of vp/cell required to produce IC50 was estimated from a dose-response nonlinear regression curve ([inhibitor] versus normalized response). Two-way ANOVA followed by Tukey's multiple comparison test was used for the analysis of IVIS bioluminescence imaging. The survival curves of the animal treatment groups were compared using the log rank test. The significance level for all tests was alpha = 0.05. The statistical analysis was performed with GraphPad Prism v8 (GraphPad Software, USA). *$p \leq 0.05$, **$p \leq 0.01$.

SUPPLEMENTAL INFORMATION

Supplemental information can be found online at https://doi.org/10.1016/j.omto.2021.12.013.

ACKNOWLEDGMENTS

The work was financially supported by Russian Foundation for Basic Research (RFBR) grant no. 18-29-01009. The work of G.M.Y. was supported by Russian Science Foundation grant no. 21-74-20110. The funder had no role in study design, data collection and analysis, decision to publish, or preparation of the manuscript. We thank Prof. Petr M. Chumakov (Engelhardt Institute of Molecular Biology, Russian Academy of Sciences, Moscow) for sharing with us human glioma cell lines and our colleagues Dr. Nadezhda Grinenko for establishing some primary glioma cultures and Dr. Victor Naumenko for help with IVIS bioluminescence imaging and analysis.

AUTHOR CONTRIBUTIONS

A.A.S., A.O.S., and V.P.C. conceived the study. A.A.S. and A.O.S. designed the study. A.A.S., A.O.S., and M.P.V. conducted the experiments, A.A.S., A.O.S., S.A.C., and A.A.C. analyzed the data. G.M.Y., Z.R., and A.V.L. contributed the resources. A.A.S. wrote the manuscript. Z.R. edited the manuscript. A.A.S. received the funding. A.A.S. and V.P.C. supervised the study. All authors have read and approved the final version of the manuscript.

DECLARATION OF INTERESTS

The authors declare no competing interests

REFERENCES

1. Stepanenko, A., and Chekhonin, V. (2018). Recent advances in oncolytic virotherapy and Immunotherapy for glioblastoma: a glimmer of hope in the search for an effective therapy? Cancers (Basel) *10*, 492.

2. Stepanenko, A.A., and Chekhonin, V.P. (2018). A compendium of adenovirus genetic modifications for enhanced replication, oncolysis, and tumor immunosurveillance in cancer therapy. Gene *679*, 11–18.

3. Stepanenko, A.A., and Chekhonin, V.P. (2018). Tropism and transduction of oncolytic adenovirus 5 vectors in cancer therapy: focus on fiber chimerism and mosaicism, hexon and pIX. Virus Res. *257*, 40–51.

4. Lu, V.M., Shah, A.H., Vallejo, F.A., Eichberg, D.G., Luther, E.M., Shah, S.S., Komotar, R.J., and Ivan, M.E. (2021). Clinical trials using oncolytic viral therapy to treat adult glioblastoma: a progress report. Neurosurg. Focus *50*, 1–8.

5. Wang, J.L., Scheitler, K.M., Wenger, N.M., and Elder, J.B. (2021). Viral therapies for glioblastoma and high-grade gliomas in adults: a systematic review. Neurosurg. Focus *50*, 1–14.

6. Lang, F.F., Conrad, C., Gomez-Manzano, C., Yung, W.K.A., Sawaya, R., Weinberg, J.S., Prabhu, S.S., Rao, G., Fuller, G.N., Aldape, K.D., et al. (2018). Phase I study of DNX-2401 (Delta-24-RGD) oncolytic adenovirus: replication and immunotherapeutic effects in recurrent malignant glioma. J. Clin. Oncol. JCO. *75*, 821.

7. Van Den Bossche, W.B.L., Kleijn, A., Teunissen, C.E., Voerman, J.S.A., Teodosio, C., Noske, D.P., Van Dongen, J.J.M., Dirven, C.M.F., and Lamfers, M.L.M. (2018). Oncolytic virotherapy in glioblastoma patients induces a tumor macrophage phenotypic shift leading to an altered glioblastoma microenvironment. Neuro. Oncol. *20*, 1494–1504.

8. Yousef, A.F., Fonseca, G.J., Pelka, P., Ablack, J.N.G., Walsh, C., Dick, F.A., Bazett-Jones, D.P., Shaw, G.S., and Mymryk, J.S. (2010). Identification of a molecular recognition feature in the E1A oncoprotein that binds the SUMO conjugase UBC9 and likely interferes with polySUMOylation. Oncogene *29*, 4693–4704.

9. Lau, L., Gray, E.E., Brunette, R.L., and Stetson, D.B. (2015). DNA tumor virus oncogenes antagonize the cGAS-STING DNA-sensing pathway. Science *350*, 568–571.

10. Fueyo, J., Gomez-Manzano, C., Alemany, R., Lee, P.S., McDonnell, T.J., Mitlianga, P., Shi, Y.X., Levin, V.A., Yung, W.K., and Kyritsis, A.P. (2000). A mutant oncolytic adenovirus targeting the Rb pathway produces anti-glioma effect in vivo. Oncogene *19*, 2–12.

11. Heise, C., Hermiston, T., Johnson, L., Brooks, G., Sampson-Johannes, A., Williams, A., Hawkins, L., and Kirn, D. (2000). An adenovirus E1A mutant that demonstrates potent and selective systemic anti-tumoral efficacy. Nat. Med. *6*, 1134–1139.

12. Sauthoff, H., Pipiya, T., Heitner, S., Chen, S., Bleck, B., Reibman, J., Chang, W., Norman, R.G., Rom, W.N., and Hay, J.G. (2004). Impact of E1a modifications on tumor-selective adenoviral replication and toxicity. Mol. Ther. *10*, 749–757.

13. Majem, M., Cascallo, M., Bayo-Puxan, N., Mesia, R., Germa, J.R., and Alemany, R. (2006). Control of E1A under an E2F-1 promoter insulated with the myotonic dystrophy locus insulator reduces the toxicity of oncolytic adenovirus Ad-Δ24RGD. Cancer Gene Ther. *13*, 696–705.

14. Balagué, C., Noya, F., Alemany, R., Chow, L.T., and Curiel, D.T. (2001). Human papillomavirus E6E7-mediated adenovirus cell killing: selectivity of mutant adenovirus replication in organotypic cultures of human keratinocytes. J. Virol. *75*, 7602–7611.

15. Kanerva, A., Bauerschmitz, G.J., Yamamoto, M., Lam, J.T., Alvarez, R.D., Siegal, G.P., Curiel, D.T., and Hemminki, A. (2004). A cyclooxygenase-2 promoter-based conditionally replicating adenovirus with enhanced infectivity for treatment of ovarian adenocarcinoma. Gene Ther. *11*, 552–559.

16. Johnson, L., Shen, A., Boyle, L., Kunich, J., Pandey, K., Lemmon, M., Hermiston, T., Giedlin, M., McCormick, F., and Fattaey, A. (2002). Selectively replicating adenoviruses targeting deregulated E2F activity are potent, systemic antitumor agents. Cancer Cell *1*, 325–337.

17. Ulasov, I.V., Tyler, M.A., Rivera, A.A., Nettlebeck, D.M., Douglas, J.T., and Lesniak, M.S. (2008). Evaluation of E1A double mutant oncolytic adenovectors in anti-glioma gene therapy. J. Med. Virol. *80*, 1595–1603.

18. Nemerow, G.R., and Stewart, P.L. (2016). Insights into adenovirus uncoating from interactions with integrins and mediators of host immunity. Viruses *8*, 337.

19. Niittykoski, M., von und zu Fraunberg, M., Martikainen, M., Rauramaa, T., Immonen, A., Koponen, S., Leinonen, V., Vähä-Koskela, M., Zhang, Q., Kühnel, F., et al. (2017). Immunohistochemical characterization and sensitivity to human adenovirus serotypes 3, 5, and 11p of new cell lines derived from human diffuse grade II to IV gliomas. Transl. Oncol. *10*, 772–779.

20. Zheng, S., Ulasov, I.V., Han, Y., Tyler, M.A., Zhu, Z.B., and Lesniak, M.S. (2007). Fiber-knob modifications enhance adenoviral tropism and gene transfer in malignant glioma. J. Gene Med. *9*, 151–160.

21. Fuxe, J., Liu, L., Malin, S., Philipson, L., Collins, V.P., and Pettersson, R.F. (2003). Expression of the coxsackie and adenovirus receptor in human astrocytic tumors and xenografts. Int. J. Cancer *103*, 723–729.

22. Skog, J., Edlund, K., Widegren, B., Salford, L.G., Wadell, G., and Mei, Y.F. (2004). Efficient internalization into low-passage glioma cell lines using adenoviruses other than type 5: an approach for improvement of gene delivery to brain tumours. J. Gen. Virol. *85*, 2627–2638.

23. Lyle, C., and McCormick, F. (2010). Integrin αvβ5 is a primary receptor for adenovirus in CAR-negative cells. Virol. J. *7*, 148.

24. Toyoda, E., Doi, R., Kami, K., Mori, T., Ito, D., Koizumi, M., Kida, A., Nagai, K., Ito, T., Masui, T., et al. (2008). Adenovirus vectors with chimeric type 5 and 35 fiber proteins exhibit enhanced transfection of human pancreatic cancer cells. Int. J. Oncol. *33*, 1141–1147.

25. Brouwer, E., Havenga, M.J., Ophorst, O., De Leeuw, B., Gijsbers, L., Gillissen, G., Hoeben, R.C., Ter Horst, M., Nanda, D., Dirven, C., et al. (2007). Human adenovirus type 35 vector for gene therapy of brain cancer: improved transduction and bypass of pre-existing anti-vector immunity in cancer patients. Cancer Gene Ther. *14*, 211–219.

26. Kolvunen, E., Wang, B., and Ruoslahti, E. (1995). Phage libraries displaying cyclic peptides with different ring sizes: ligand specificities of the rgd-directed integrine. Bio/Technology *13*, 265–270.

27. Dmitriev, I., Krasnykh, V., Miller, C.R., Wang, M., Kashentseva, E., Mikheeva, G., Belousova, N., and Curiel, D.T. (1998). An adenovirus vector with genetically modified fibers demonstrates expanded tropism via utilization of a coxsackievirus and adenovirus receptor-independent cell entry mechanism. J. Virol. *72*, 9706–9713.

28. Suzuki, K., Fueyo, J., Krasnykh, V., Reynolds, P.N., Curiel, D.T., and Alemany, R. (2001). A conditionally replicative adenovirus with enhanced infectivity shows improved oncolytic potency. Clin. Cancer Res. *7*, 120–126.

29. Lamfers, M.L.M., Grill, J., Dirven, C.M.F., Van Beusechem, V.W., Geoerger, B., Van Den Berg, J., Alemany, R., Fueyo, J., Curiel, D.T., Vassal, G., et al. (2002). Potential of the conditionally replicative adenovirus Ad5-Delta24RGD in the treatment of malignant gliomas and its enhanced effect with radiotherapy. Cancer Res. *62*, 5736–5742.

30. Fueyo, J., Alemany, R., Gomez-Manzano, C., Fuller, G.N., Khan, A., Conrad, C.A., Liu, T.J., Jiang, H., Lemoine, M.G., Suzuki, K., et al. (2003). Preclinical characterization of the antiglioma activity of a tropism-enhanced adenovirus targeted to the retinoblastoma pathway. J. Natl. Cancer Inst. *95*, 652–660.

31. Yoon, A.-R., Hong, J., Kim, S.W., and Yun, C.-O. (2016). Redirecting adenovirus tropism by genetic, chemical, and mechanical modification of the adenovirus surface for cancer gene therapy. Expert Opin. Drug Deliv. *13*, 1–16.

32. Yang, M., Yang, C.S., Guo, W., Tang, J., Huang, Q., Feng, S., Jiang, A., Xu, X., Jiang, G., and Liu, Y.Q. (2017). A novel fiber chimeric conditionally replicative adenovirus-Ad5/F35 for tumor therapy. Cancer Biol. Ther. *18*, 833–840.

33. Wang, H., Li, Z.-Y., Liu, Y., Persson, J., Beyer, I., Möller, T., Koyuncu, D., Drescher, M.R., Strauss, R., Zhang, X.-B., et al. (2011). Desmoglein 2 is a receptor for adenovirus serotypes 3, 7, 11 and 14. Nat. Med. *17*, 96–104.

34. Trinh, H.V., Lesage, G., Chennamparampil, V., Vollenweider, B., Burckhardt, C.J., Schauer, S., Havenga, M., Greber, U.F., and Hemmi, S. (2012). Avidity binding of human adenovirus serotypes 3 and 7 to the membrane cofactor CD46 triggers infection. J. Virol. *86*, 1623–1637.

35. Gaggar, A., Shayakhmetov, D.M., and Lieber, A. (2003). CD46 is a cellular receptor for group B adenoviruses. Nat. Med. *9*, 1408–1412.

36. Hensen, L.C.M., Hoeben, R.C., and Bots, S.T.F. (2020). Adenovirus receptor expression in cancer and its multifaceted role in oncolytic adenovirus therapy. Int. J. Mol. Sci. *21*, 1–22.

37. Volk, A.L., Rivera, A.A., Kanerva, A., Bauerschmitz, G., Dmitriev, I., Nettelbeck, D.M., and Curiel, D.T. (2003). Enhanced adenovirus infection of melanoma cells by fiber-modification: incorporation of RGD peptide or Ad5/3 chimerism. Cancer Biol. Ther. *2*, 511–515.

38. Stoff-Khalili, M.A., Stoff, A., Rivera, A.A., Mathis, J.M., Everts, M., Wang, M., Kawakami, Y., Waehler, R., Mathews, Q.L., Yamamoto, M., et al. (2005). Gene transfer to carcinoma of the breast with fiber-modified adenoviral vectors in a tissue slice model system. Cancer Biol. Ther. *4*, 1203–1210.

39. Guse, K., Ranki, T., Ala-Opas, M., Bono, P., Särkioja, M., Rajecki, M., Kanerva, A., Hakkarainen, T., and Hemminki, A. (2007). Treatment of metastatic renal cancer with capsid-modified oncolytic adenoviruses. Mol. Cancer Ther. *6*, 2728–2736.

40. Kangasniemi, L., Kiviluoto, T., Kanerva, A., Raki, M., Ranki, T., Sarkioja, M., Wu, H., Marini, F., Höckerstedt, K., Isoniemi, H., et al. (2006). Infectivity-enhanced adenoviruses deliver efficacy in clinical samples and orthotopic models of disseminated gastric cancer. Clin. Cancer Res. *12*, 3137–3144.

41. Davydova, J., Le, L.P., Gavrikova, T., Wang, M., Krasnykh, V., and Yamamoto, M. (2004). Infectivity-enhanced cyclooxygenase-2-based conditionally replicative adenoviruses for esophageal adenocarcinoma treatment. Cancer Res. *64*, 4319–4327.

42. Borovjagin, A.V., Krendelchtchikov, A., Ramesh, N., Yu, D.-C., Douglas, J.T., and Curiel, D.T. (2005). Complex mosaicism is a novel approach to infectivity enhancement of adenovirus type 5-based vectors. Cancer Gene Ther. *12*, 475–486.

43. Nandi, S., Ulasov, I.V., Rolle, C.E., Han, Y., and Lesniak, M.S. (2009). A chimeric adenovirus with an Ad 3 fiber knob modification augments glioma virotherapy. J. Gene Med. *11*, 1005–1011.

44. Hoffmann, D., Bayer, W., Heim, A., Potthoff, A., Nettelbeck, D.M., and Wildner, O. (2008). Evaluation of twenty-one human adenovirus types and one infectivity-enhanced adenovirus for the treatment of malignant melanoma. J. Invest. Dermatol. *128*, 988–998.

45. Hoffmann, D., Heim, A., Nettelbeck, D.M., Steinstraesser, L., and Wildner, O. (2007). Evaluation of twenty human adenoviral types and one infectivity-enhanced adenovirus for the therapy of soft tissue sarcoma. Hum. Gene Ther. *18*, 51–62.

46. Hoffman, D., Meyer, B., and Wildner, O. (2007). Improved glioblastoma treatment with Ad5/35 fiber chimeric conditionally replicating adenoviruses. J. Gene Med. *9*, 764–778.

47. Tyler, M.A., Ulasov, I.V., Borovjagin, A., Sonabend, A.M., Khramtsov, A., Han, Y., Dent, P., Fisher, P.B., Curiel, D.T., and Lesniak, M.S. (2006). Enhanced transduction of malignant glioma with a double targeted Ad5/3-RGD fiber-modified adenovirus. Mol. Cancer Ther. *5*, 2408–2416.

48. Dobbins, G.C., Ugai, H., Curiel, D.T., and Gillespie, G.Y. (2015). A multi targeting conditionally replicating adenovirus displays enhanced oncolysis while maintaining expression of immunotherapeutic agents. PLoS One *10*, e0145272.

49. Krasnykh, V.N., Mikheeva, G.V., Douglas, J.T., and Curiel, D.T. (1996). Generation of recombinant adenovirus vectors with modified fibers for altering viral tropism. J. Virol. *70*, 6839–6846.

50. Shayakhmetov, D.M., Papayannopoulou, T., Stamatoyannopoulos, G., and Lieber, A. (2000). Efficient gene transfer into human CD34(+) cells by a retargeted adenovirus vector. J. Virol. *74*, 2567–2583.

51. Matsui, H., Sakurai, F., Kurachi, S., Tashiro, K., Sugio, K., Kawabata, K., Yamanishi, K., and Mizuguchi, H. (2009). Development of fiber-substituted adenovirus vectors containing foreign peptides in the adenovirus serotype 35 fiber knob. Gene Ther. *16*, 1050–1057.

52. Puigdelloses, M., Garcia-Moure, M., Labiano, S., Laspidea, V., Gonzalez-Huarriz, M., Zalacain, M., Marrodan, L., Martinez-Velez, N., De La Nava, D., Ausejo, I., et al. (2021). CD137 and PD-L1 targeting with immunovirotherapy induces a potent and durable antitumor immune response in glioblastoma models. J. Immunother. Cancer *9*, e002644.

53. Jiang, H., Rivera-Molina, Y., Gomez-Manzano, C., Clise-Dwyer, K., Bover, L., Vence, L.M., Yuan, Y., Lang, F.F., Toniatti, C., Hossain, M.B., et al. (2017). Oncolytic adenovirus and tumor-targeting immune modulatory therapy improve autologous cancer vaccination. Cancer Res. *77*, 3894–3907.

54. Rivera-Molina, Y., Jiang, H., Fueyo, J., Nguyen, T., Shin, D.H., Youssef, G., Fan, X., Gumin, J., Alonso, M.M., Phadnis, S., et al. (2019). GITRL-armed Delta-24-RGD oncolytic adenovirus prolongs survival and induces anti-glioma immune memory. Neurooncol. Adv. *1*, vdz009.

55. Rajecki, M., Kanerva, A., Stenman, U.H., Tenhunen, M., Kangasniemi, L., Särkioja, M., Ala-Opas, M.Y., Alfthan, H., Sankila, A., Rintala, E., et al. (2007). Treatment of prostate cancer with Ad5/3Δ24hCG allows non-invasive detection of the magnitude and persistence of virus replication in vivo. Mol. Cancer Ther. *6*, 742–751.

56. Lv, Y., Xiao, F.J., Wang, Y., Zou, X.H., Wang, H., Wang, H.Y., Wang, L.S., and Lu, Z.Z. (2019). Efficient gene transfer into T lymphocytes by fiber-modified human adenovirus 5. BMC Biotechnol. *19*, 23.

57. Hesse, A., Kosmides, D., Kontermann, R.E., and Nettelbeck, D.M. (2007). Tropism modification of adenovirus vectors by peptide ligand insertion into various positions of the adenovirus serotype 41 short-fiber knob domain. J. Virol. *81*, 2688–2699.

58. Rivera, A.A., Davydova, J., Schierer, S., Wang, M., Krasnykh, V., Yamamoto, M., Curiel, D.T., and Nettelbeck, D.M. (2004). Combining high selectivity of replication with fiber chimerism for effective adenoviral oncolysis of CAR-negative melanoma cells. Gene Ther. *11*, 1694–1702.

59. Geoerger, B., Vassal, G., Opolon, P., Dirven, C.M.F., Morizet, J., Laudani, L., Grill, J., Giaccone, G., Vandertop, W.P., Gerritsen, W.R., et al. (2004). Oncolytic activity of p53-expressing conditionally replicative adenovirus AdΔ24-p53 against human malignant glioma. Cancer Res. *64*, 5753–5759.

60. Sohn, S.Y., and Hearing, P. (2019). Adenoviral strategies to overcome innate cellular responses to infection. FEBS Lett. *593*, 3484–3495.

61. Miller, C.R., Buchsbaum, D.J., Reynolds, P.N., Douglas, J.T., Gillespie, G.Y., Mayo, M.S., Raben, D., and Curiel, D.T. (1998). Differential susceptibility of primary and established human glioma cells to adenovirus infection: targeting via the epidermal growth factor receptor achieves fiber receptor-independent gene transfer. Cancer Res. *58*, 5738–5748.

62. Asaoka, K., Tada, M., Sawamura, Y., Ikeda, J., and Abe, H. (2000). Dependence of efficient adenoviral gene delivery in malignant glioma cells on the expression levels of the Coxsackievirus and adenovirus receptor. J. Neurosurg. *92*, 1002–1008.

63. Yu, L., Shimozato, O., Li, Q., Kawamura, K., Ma, G., Namba, M., Ogawa, T., Kaiho, I., and Tagawa, M. (2007). Adenovirus type 5 substituted with type 11 or 35 fiber structure increases its infectivity to human cells enabling dual gene transfer in CD46-dependent and -independent manners. Anticancer Res. *27*, 2311–2316.

64. Yu, L., Takenobu, H., Shimozato, O., Kawamura, K., Nimura, Y., Seki, N., Uzawa, K., Tanzawa, H., Shimada, H., Ochiai, T., et al. (2005). Increased infectivity of adenovirus type 5 bearing type 11 or type 35 fibers to human esophageal and oral carcinoma cells. Oncol. Rep. *14*, 831–835.

65. Cho, Y.S., Do, M.H., Kwon, S.Y., Moon, C., Kim, K., Lee, K., Lee, S.J., Hemmi, S., Joo, Y.E., Kim, M.S., et al. (2016). Efficacy of CD46-targeting chimeric Ad5/35 adenoviral gene therapy for colorectal cancers. Oncotarget *7*, 38210–38223.

66. Drouin, M., Cayer, M.-P., and Jung, D. (2010). Adenovirus 5 and chimeric adenovirus 5/F35 employ distinct B-lymphocyte intracellular trafficking routes that are independent of their cognate cell surface receptor. Virology *401*, 305–313.

67. Donovan-Banfield, I., Turnell, A.S., Hiscox, J.A., Leppard, K.N., and Matthews, D.A. (2020). Deep splicing plasticity of the human adenovirus type 5 transcriptome drives virus evolution. Commun. Biol. *3*, 124.

68. Stepanova, O.V., Voronova, A.D., Chadin, A.V., Valikhov, M.P., Semkina, A.S., Karsuntseva, E.K., Chekhonin, I.V., Shishkina, V.S., Reshetov, I.V., and Chekhonin, V.P. (2019). Efficiency of human olfactory ensheathing cell transplantation into spinal cysts to improve mobility of the hind limbs. Stem Cells Dev. *28*, 1253–1263.

69. Zhang, W., Fu, J., and Ehrhardt, A. (2018). Novel vector construction based on alternative adenovirus types via homologous recombination. Hum. Gene Ther. Methods *29*, 124–134.

70. Shi, Z., and Vickers, C.E. (2016). Molecular Cloning Designer Simulator (MCDS): all-in-one molecular cloning and genetic engineering design, simulation and management software for complex synthetic biology and metabolic engineering projects. Metab. Eng. Commun. *3*, 173–186.

71. Peng, H.H., Wu, S., Davis, J.J., Wang, L., Roth, J.A., Marini, F.C., and Fang, B. (2006). A rapid and efficient method for purification of recombinant adenovirus with arginine-glycine-aspartic acid-modified fibers. Anal. Biochem. *354*, 140–147.

72. Stepanenko, A.A., Sosnovtseva, A.O., Valikhov, M.P., and Chekhonin, V.P. (2021). A new insight into aggregation of oncolytic adenovirus Ad5-delta-24-RGD during CsCl gradient ultracentrifugation. Sci. Rep. *11*, 16088.

73. Giménez-Alejandre, M., Gros, A., and Alemany, R. (2012). Construction of capsid-modified adenoviruses by recombination in yeast and purification by iodixanol-gradient. In Methods in Molecular Biology (Humana Press Inc.), pp. 21–34.

74. Gallaher, S.D., and Berk, A.J. (2013). A rapid Q-PCR titration protocol for adenovirus and helper-dependent adenovirus vectors that produces biologically relevant results. J. Virol. Methods *192*, 28–38.

75. Rocha, N., Bulger, D.A., Frontini, A., Titheradge, H., Gribsholt, S.B., Knox, R., Page, M., Harris, J., Payne, F., Adams, C., et al. (2017). Human biallelic MFN2 mutations induce mitochondrial dysfunction, upper body adipose hyperplasia, and suppression of leptin expression. Elife *6*, e23813.